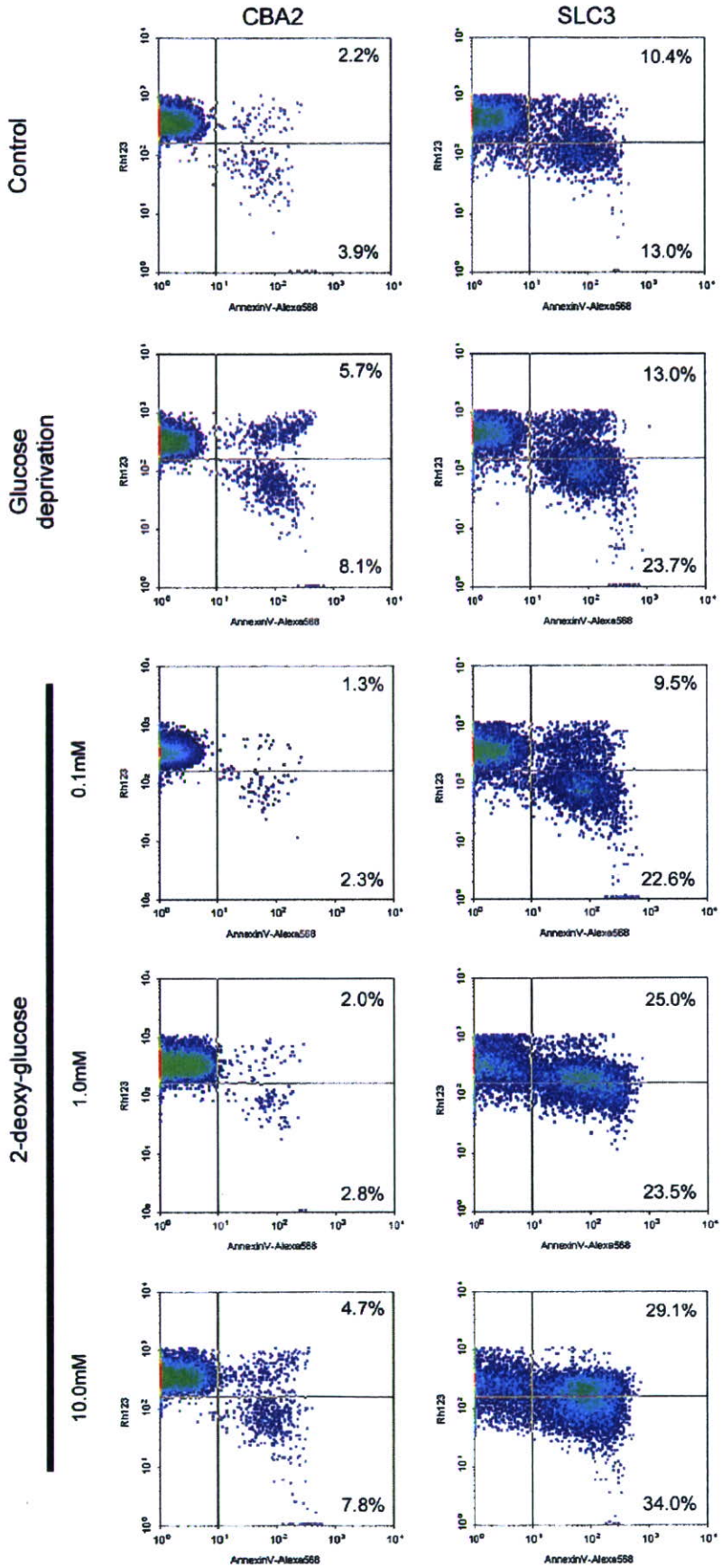
CBA2
SLC3
Control
Glucose deprivation
2-deoxy-glucose
0.1mM
1.0mM
10.0mM
2.2%
3.9%
10.4%
13.0%
5.7%
8.1%
13.0%
23.7%
1.3%
2.3%
9.5%
22.6%
2.0%
2.8%
25.0%
23.5%
4.7%
7.8%
29.1%
34.0%
Rh123
AnnexinV-Alexa568

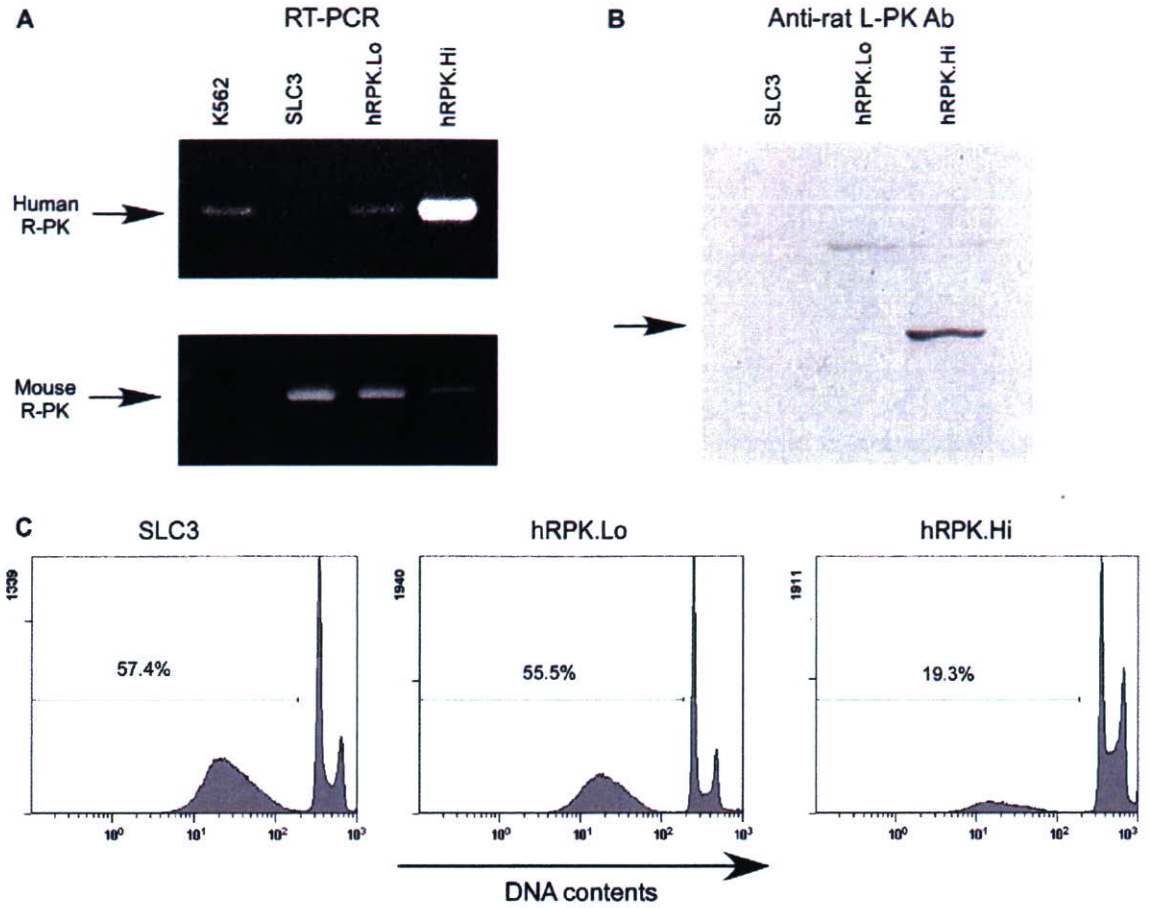

Figure 2. Establishment of the transfectants, SLC3-hRPK.Hi (hRPK.Hi) and SLC3.hRPK.Lo (hRPK.Lo), by introducing the human red blood cell type-pyruvate kinase (R-PK) gene into murine R-PK–deficient cells. Transgene-expression was confirmed by reverse transcriptase polymerase chain reaction (**A**) and Western blotting (**B**). The expression level of hRPK.Hi was higher than that of hRPK.Lo. (**C**) Apoptosis induction in the PK-deficient cells and transfectants. Transfected human R-PK recovered the glycolytic function and showed reduced spontaneous apoptotic changes. The numbers in figures represent the apoptotic change ratio.

forced overexpression of the PK gene reduced intracellular ROS in an expression-level dependent manner (Fig. 5C).

Discussion

Overexpression of human R-PK in SLC3 results in the reduction of apoptotic cells (Fig. 2C), and DNA microarray analysis showed that genes involved in the cell cycle, DNA repair, and antioxidants were downregulated. In general, gene expression levels of transfectants were lower than that of SLC3 (Fig. 3). However, aberrant apoptosis and invalid cell proliferation were restrained in the transfectants. These observations suggested that the cellular activity was not suppressed but was reverted to the normal level by the transgene. It is most likely that the candidate genes suppressed in transfectants were induced in R-PK mutant cells.

Although there were several candidate genes attributing to apoptosis-induction in SLC3, it was still unclear whether these genes were associated with each other or independent. However, there was a possibility that a signal cross-talk phenomenon occurred [14]. *Bad*, a gene encoding a member of the Bcl2-family proapoptotic molecules in mitochondria was significantly downregulated by the transgene (Figs. 3A and 4). Danial et al. [15] reported that *Bad*, BCL2-antagonist of cell death, formed a functional holoenzyme complex together with several molecules, such as glucokinase (hexokinase-4) in liver mitochondria, and contributed to apoptosis induction by glucose deprivation. Our observation suggested that *Bad*

Figure 1. Apoptosis induced by glycolytic inhibition in erythroid cell lines. Glucose deprivation or exposure to 2-deoxyglucose inhibits glycolysis and finally causes apoptosis. The red blood cell type-pyruvate kinase (R-PK)–deficient erythroid cell line (SLC3) is more susceptible than wild-type cells (CBA2) in these conditions. The horizontal axis shows AnnexinV-Arexa568 (= apoptotic change) and the vertical axis shows Rhodamin123 fluorescence (= mitochondrial membrane potential).

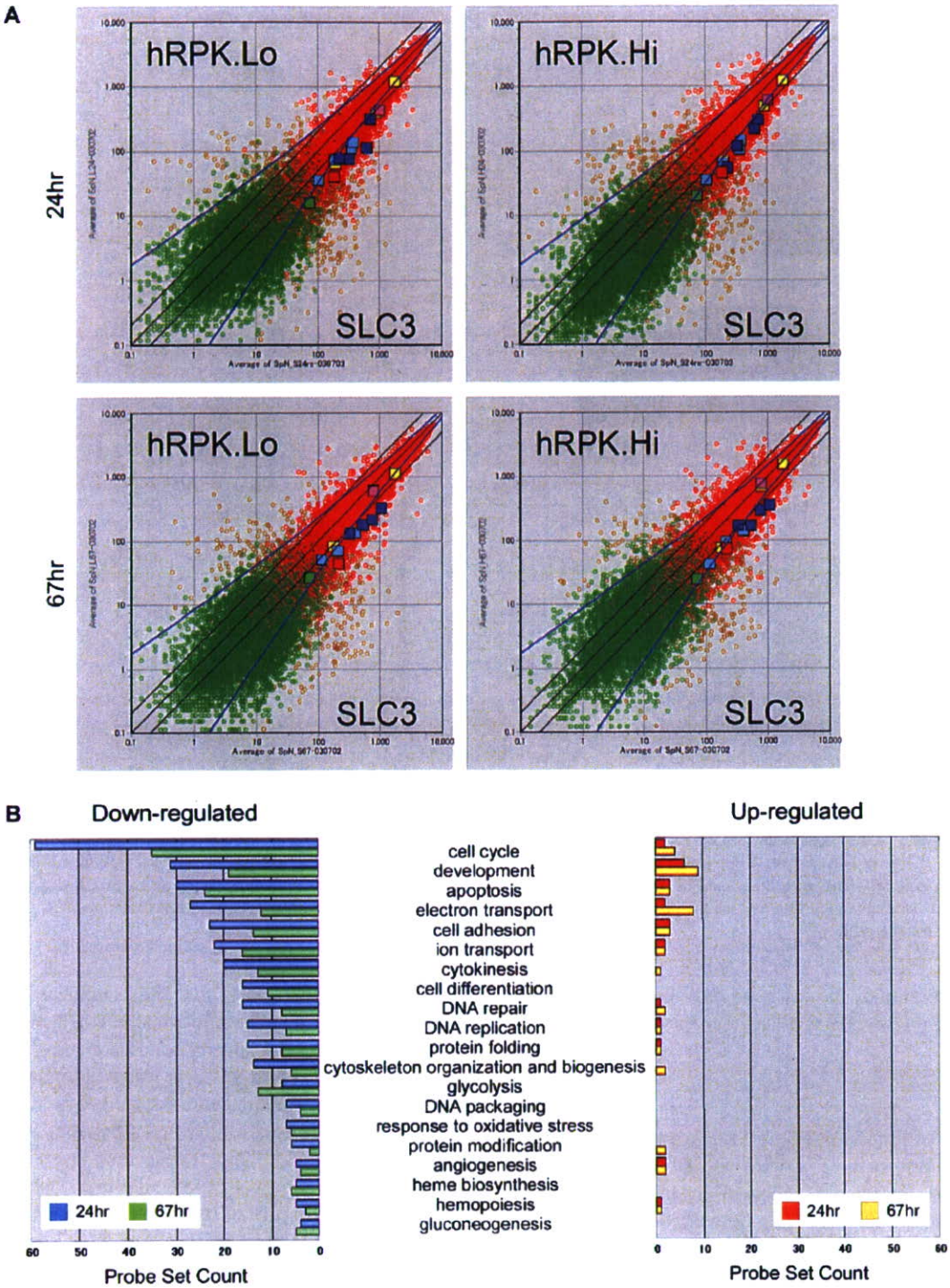

Figure 3. Genome-wide expression analysis of the glycolysis defect. Analysis was performed using the Affymetrix GeneChip Mouse Expression Array 430A, which contains about 20,000 genes. **(A)** Scatter plot between SLC3 and hRPK transfectants at 24 or 67 hours. The open circle shows the expression level of every probe set. The color shows these probabilities provided by the Affymetrix GeneChip Operation System: red means good and green means poor. The colored squares show *Bad* (red), *Bnip3* and *Bnip3l* (blue), *hif1a* (green), *Brca1* and *Brca2* (aqua), *Prdx1* (pink) and *Txnl1* (yellow), respectively. The black lines show twofold, onefold, and 0.5-fold, respectively, and the blue lines show the empirical threshold level. **(B)** The categorized aggregate graph. All probe sets were categorized by the Biological Process Ontology keywords provided by the Gene Ontology project (http://www.geneontology.org/). Up- or downregulation was determined by the spot location in the scatter plotting. Compared with the empirical threshold lines, the upper spots show upregulated genes and the lower spots show downregulated genes.

A Down-regulated Genes

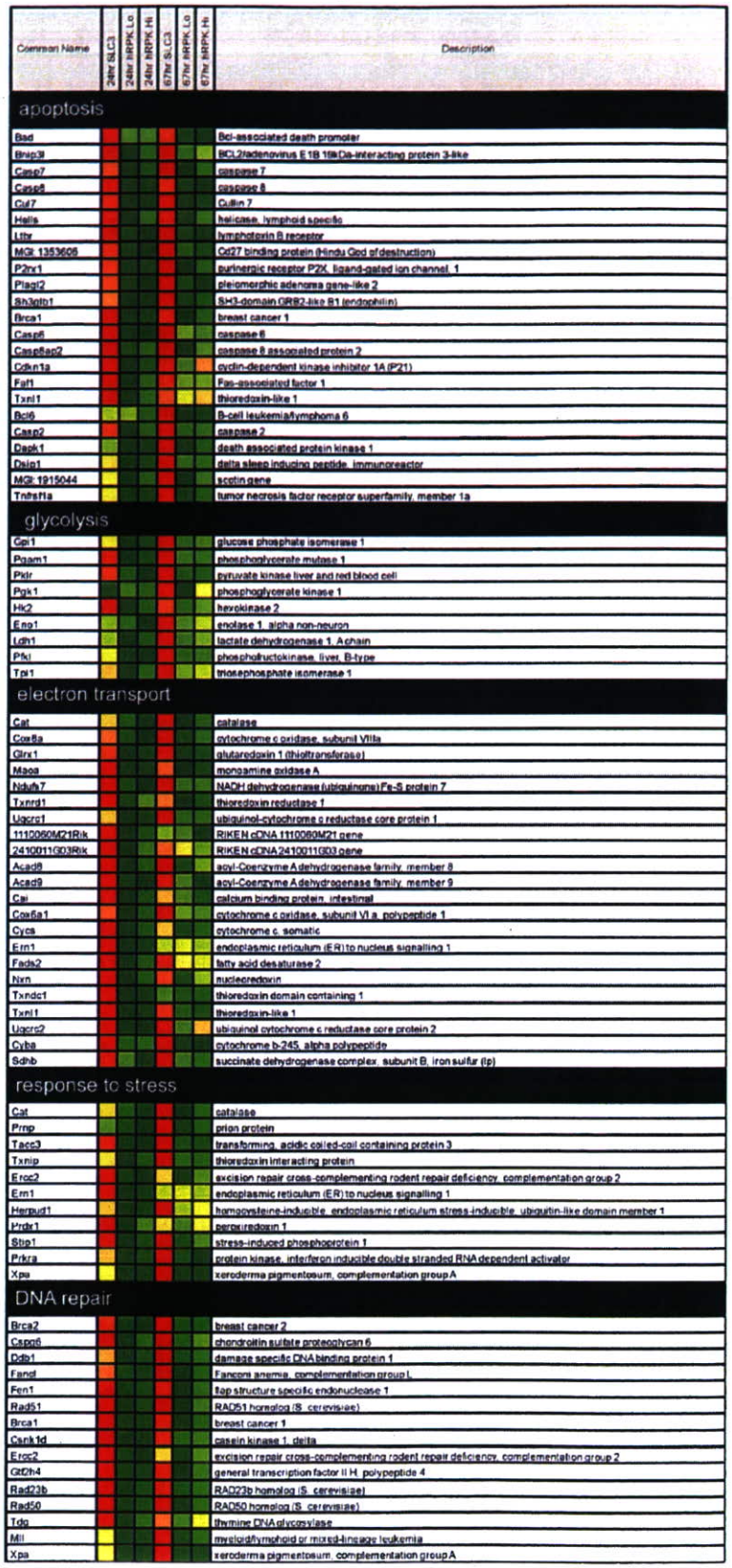

Common Name	24hr SLC3	24hr ARPK Lo	24hr ARPK Hi	67hr SLC3	67hr ARPK Lo	67hr ARPK Hi	Description
apoptosis							
Bad							Bcl-associated death promoter
Bnip3l							BCL2/adenovirus E1B 19kDa-interacting protein 3-like
Casp7							caspase 7
Casp8							caspase 8
Cul7							Cullin 7
Hells							helicase, lymphoid specific
Ltbr							lymphotoxin B receptor
MGI:1353606							Cd27 binding protein (Hindu God of destruction)
P2rx1							purinergic receptor P2X, ligand-gated ion channel, 1
Plagl2							pleiomorphic adenoma gene-like 2
Sh3gb1							SH3-domain GRB2-like B1 (endophilin)
Brca1							breast cancer 1
Casp6							caspase 6
Casp8ap2							caspase 8 associated protein 2
Cdkn1a							cyclin-dependent kinase inhibitor 1A (P21)
Faf1							Fas-associated factor 1
Txnl1							thioredoxin-like 1
Bcl6							B-cell leukemia/lymphoma 6
Casp2							caspase 2
Dapk1							death associated protein kinase 1
Dsip1							delta sleep inducing peptide, immunoreactor
MGI:1915044							scotin gene
Tnfrsf1a							tumor necrosis factor receptor superfamily, member 1a
glycolysis							
Gpi1							glucose phosphate isomerase 1
Pgam1							phosphoglycerate mutase 1
Pklr							pyruvate kinase liver and red blood cell
Pgk1							phosphoglycerate kinase 1
Hk2							hexokinase 2
Eno1							enolase 1, alpha non-neuron
Ldh1							lactate dehydrogenase 1, A chain
Pfkl							phosphofructokinase, liver, B-type
Tpi1							triosephosphate isomerase 1
electron transport							
Cat							catalase
Cox8a							cytochrome c oxidase, subunit VIIIa
Glrx1							glutaredoxin 1 (thioltransferase)
Maoa							monoamine oxidase A
Ndufs7							NADH dehydrogenase (ubiquinone) Fe-S protein 7
Txnrd1							thioredoxin reductase 1
Uqcrc1							ubiquinol-cytochrome c reductase core protein 1
1110060M21Rik							RIKEN cDNA 1110060M21 gene
2410011G03Rik							RIKEN cDNA 2410011G03 gene
Acad8							acyl-Coenzyme A dehydrogenase family, member 8
Acad9							acyl-Coenzyme A dehydrogenase family, member 9
Cai							calcium binding protein, intestinal
Cox5a1							cytochrome c oxidase, subunit V1a, polypeptide 1
Cycs							cytochrome c, somatic
Ern1							endoplasmic reticulum (ER) to nucleus signalling 1
Fads2							fatty acid desaturase 2
Nxn							nucleoredoxin
Txndc1							thioredoxin domain containing 1
Txnl1							thioredoxin-like 1
Uqcrc2							ubiquinol cytochrome c reductase core protein 2
Cyba							cytochrome b-245, alpha polypeptide
Sdhb							succinate dehydrogenase complex, subunit B, iron sulfur (Ip)
response to stress							
Cat							catalase
Prnp							prion protein
Tacc3							transforming, acidic coiled-coil containing protein 3
Txnip							thioredoxin interacting protein
Ercc2							excision repair cross-complementing rodent repair deficiency, complementation group 2
Ern1							endoplasmic reticulum (ER) to nucleus signalling 1
Herpud1							homocysteine-inducible, endoplasmic reticulum stress-inducible, ubiquitin-like domain member 1
Prdx1							peroxiredoxin 1
Stip1							stress-induced phosphoprotein 1
Prkra							protein kinase, interferon inducible double stranded RNA dependent activator
Xpa							xeroderma pigmentosum, complementation group A
DNA repair							
Brca2							breast cancer 2
Cspg6							chondroitin sulfate proteoglycan 6
Ddb1							damage specific DNA binding protein 1
Fancl							Fanconi anemia, complementation group L
Fen1							flap structure specific endonuclease 1
Rad51							RAD51 homolog (S. cerevisiae)
Brca1							breast cancer 1
Csnk1d							casein kinase 1, delta
Ercc2							excision repair cross-complementing rodent repair deficiency, complementation group 2
Gtf2h4							general transcription factor II H, polypeptide 4
Rad23b							RAD23b homolog (S. cerevisiae)
Rad50							RAD50 homolog (S. cerevisiae)
Tdg							thymine DNA glycosylase
Mll							myeloid/lymphoid or mixed-lineage leukemia
Xpa							xeroderma pigmentosum, complementation group A

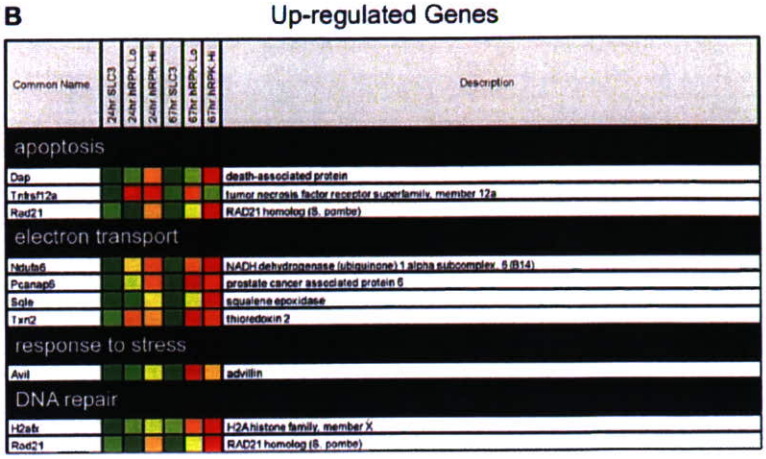

Figure 4. *Continued*

could be involved in the apoptosis induced by glycolysis defect in erythroid cells as well as in the liver.

The genes of apoptosis-inducers related to hypoxia such as *Bnip3* and *Bnip3l*, which are known as inducible genes by hypoxia-inducible factor-1α, were inactivated markedly by the forced expression of the wild-type R-PK gene. Although the extent of downregulation was smaller than for *Bnip3*, *Bnip3l* showed a significant decrease of expression by the transgene (Fig. 3A). Moreover, the downregulation was more obvious at 24 hours, suggesting that these genes may contribute to the initial response caused by a glycolytic defect. These observations strongly suggested that the apoptosis induction by the glycolysis disorder was executed by the *Bnip3-Bnip3l* signal.

It is noticeable that several genes important for responding to oxidative stress are upregulated, suggesting that R-PK deficiency might account for intracellular ROS production. This speculation is supported by the following experimental observations: Firstly, SLC3 cells were more sensitive to glycolytic inhibitions such as glucose deprivation and supplementation with 2-DG (Fig. 1), and these conditions induced ROS production detected by DCFH-DA (Fig. 5A). Apoptotic changes induced by 2-DG were partly rescued by preincubation with the glutathione precursor (Fig. 5B). Finally, transgene expression reduced intracellular ROS in an expression-level–dependent manner (Fig. 5C).

Glycolytic disorders may cause cellular conditions similar to those of hypoxia. Shim et al. [16] reported that induction of the LDH-A gene by c-Myc was advantageous to transformed cells that exist under hypoxic conditions [15]. However, glucose deprivation induces the extensive apoptosis of cells overexpressing c-Myc. Overexpression of LDH-A alone in fibroblasts is sufficient to sensitize cells to this glucose deprivation-induced apoptosis. They proposed a hypothesis that LDH-A was a downstream target of c-Myc that mediates this unique apoptotic phenotype. We noticed that pyruvate was the final product as well as the substrate of the PK and LDH reaction, respectively. Both LDH hyperactivity and PK deficiency may cause the depletion of intracellular pyruvate, suggesting that pyruvate has an important role in preventing apoptosis.

Several studies have revealed that pyruvate acts as an antioxidant and that PK has a protective role against oxidative stress in this respect. Brand et al. [17] reported that proliferating thymocytes mainly depend on energy derived from aerobic glycolysis, and that their sensitivity to 12-myristate 13-acetate–induced ROS production is much lower than that of resting thymocytes, which produce ATP mainly through oxidative phosphorylation. They suggested that pyruvate functions as an ROS scavenger, because the incubation of proliferating thymocytes with pyruvate reduced ROS formation.

The PK-overexpressing neuronal cells could attenuate oxidative stress and maintain cell viability [18]. Lee et al. [19] showed that hydrogen peroxide depleted intracellular GSH in human umbilical vein endothelial cells, and that was prevented by pyruvate but not by L-lactate or aminooxyacetate. The activation of caspases was strongly inhibited by pyruvate, but markedly enhanced by L-lactate and aminooxyacetate, implicating the redox-related antiapoptotic mechanisms of pyruvate. Myocardial ischemia-reperfusion

Figure 4. Representative list of the genes affected by the functional recovery of glycolysis. Genome-wide expression analysis was performed using Affymetrix GeneChip Mouse Expression Array 430A, which contains about 20,000 genes. In the comparison among hRPK.Hi, hRPK.Lo, and SLC3, about 6000 genes were downregulated and about 500 genes were upregulated by the functional recovery of glycolysis at 24 and/or 67 hours after regular passage. These lists contain the affected genes related to apoptosis and/or the oxidative stress response.

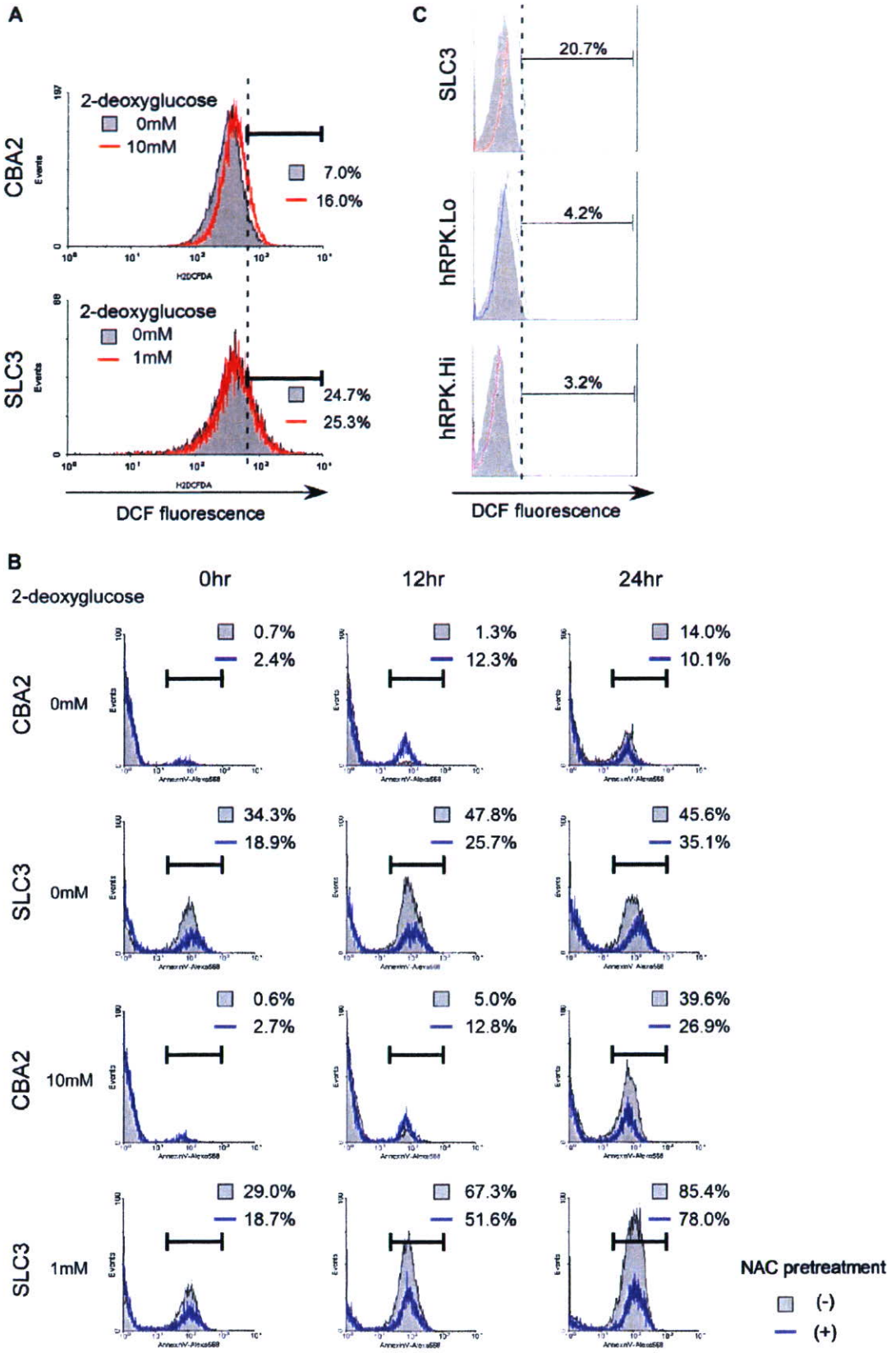
A
CBA2
2-deoxyglucose
0mM
10mM
7.0%
16.0%
SLC3
2-deoxyglucose
0mM
1mM
24.7%
25.3%
H2DCFDA
DCF fluorescence
C
SLC3
20.7%
hRPK.Lo
4.2%
hRPK.Hi
3.2%
DCF fluorescence
B
2-deoxyglucose
0hr
12hr
24hr
CBA2
0mM
0.7%
2.4%
1.3%
12.3%
14.0%
10.1%
SLC3
0mM
34.3%
18.9%
47.8%
25.7%
45.6%
35.1%
CBA2
10mM
0.6%
2.7%
5.0%
12.8%
39.6%
26.9%
SLC3
1mM
29.0%
18.7%
67.3%
51.6%
85.4%
78.0%
NAC pretreatment
(-)
(+)

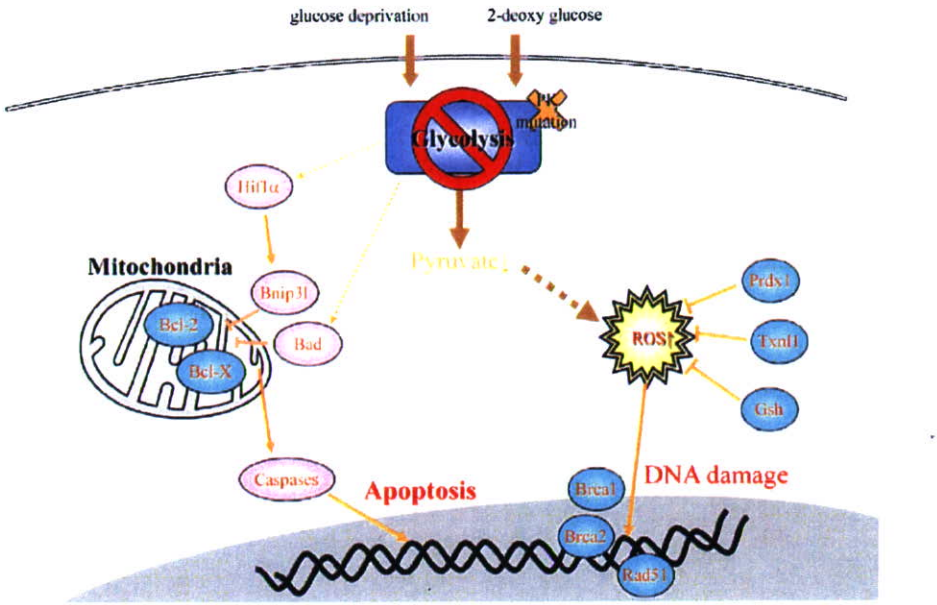

Figure 6. Glycolytic defect causes oxidative stress and hypoxia-like signal activation. Pyruvate, which is final metabolic product of the glycolytic pathway, acts as an antioxidant. Therefore, glycolytic defect elevates intracellular reactive oxygen species (ROS) and causes cellular damage, such as DNA damage and lipid oxidation. At the same time, glycolytic defect is most likely to activate signal transduction through hypoxia-inducible factor-1α (HIF-1α). These cellular responses could be accountable for the apoptosis induced by glycolytic defect.

is reported to be associated with bursts of ROS, such as superoxide radicals, and cardiac superoxide formation can be inhibited by pyruvate [20]. Thus cytotoxicities due to cardiac ischemia-reperfusion ROS can be alleviated by redox reactants such as pyruvate. These results support our present data, which showed that a mutation of the PK gene as well as inhibition of glycolysis by 2-DG augmented intracellular ROS of erythroid cells, leading to apoptosis. Introduction of the wild-type PK gene into SLC3 cells partly reduced ROS and apoptosis (Figs. 2C and 6C).

In human RBC, the most important antioxidant is GSH. Mutations of enzymes involving the synthesis and reduction of GSH, such as γ-glutamylcystein synthetase, GSH-S, glutathione reductase, and glucose-6-phosphate dehydrogenase account for the shortened RBC survival [1,21]. Recently, Neumann et al. [22] and Lee et al. [23] reported the essential roles of both peroxiredoxin (Prdx) 1 and 2 in RBC protection from oxidative stress. The hemolytic anemia of mice with targeted inactivation of *Prdx1* is characterized by an increase in erythrocyte reactive oxygen species, leading to protein oxidation and Heinz body formation. Similarly, the *Prdx2* knockout mice had Heinz body-positive hemolytic anemia with splenomegaly. The dense RBC fractions contained markedly higher levels of ROS. These studies highlighted a pivotal role of *Prdx* as a scavenger of hydrogen peroxide in RBC. *Prdx1* may be concerned with the initial response to glycolytic deficiency, because the gene expression in SLC3 was higher than that in transfectants only at 24 hours (Fig. 3A). The mechanisms responsible for upregulation of *Prdx1* and similar antioxidant enzymes in SLC3 remain to be elucidated.

It is most likely that the main pathogenesis of PK deficiency is decreased ATP production due to impaired glycolysis, resulting in the premature destruction of RBC in the reticuloendothelial system, i.e., extravascular hemolysis. In most cases, hemolysis is partly compensated by enhanced erythropoiesis. We have previously shown that the numbers of hematopoietic progenitors including colony-forming unit (CFU)-erythroid, CFU-granulocyte macrophage, burst-forming unit-erythroid, and CFU-granulocyte-erythrocyte monocyte-megakaryocyte were increased in *Pk-1*^{slc} mice [10]. The proliferation of erythroid progenitors might require

Figure 5. The oxidative stress pathway might play some role in the apoptosis induced by glycolytic disorder. (**A**) The SLC3 cells produce 2′,7′-dichlorofluorescein (DCF) continuously with and without 2-deoxyglucose (2-DG) due to the red blood cell type-pyruvate kinase (R-PK) defect. The control CBA2 cells produce DCF with 10 mM 2-DG for 30 minutes. The gray area shows the nontreated group and the red line shows the treated group with 2-DG. The horizontal axis shows the fluorescence intensity of the DCF. (**B**) The apoptosis induced by glycolytic defect or by glycolysis inhibitor was suppressed by the preincubation with the glutathione precursor, N-acetyl-cysteine (NAC). The gray area shows the nonpretreated group and the blue line shows the pretreated group with NAC. The horizontal axis shows the fluorescence intensity of the Annexin V-Alexa568.

activation of glycolysis in order to suppress intracellular ROS. Therefore, R-PK deficiency becomes a serious problem for erythroid cells to avoid apoptosis. In summary, we concluded that the premature destruction of RBC as well as apoptosis of erythroid progenitors accounts for the pathogenesis of R-PK deficiency.

Although most severe cases die either in utero or during the neonatal period [24,25], there is no curative therapy of PK deficiency except hematopoietic stem cell transplantation [26] at present. Because hematopoietic stem cell transplantation may accompany life-threatening complications, a safer treatment should be considered. Studies on the apoptotic induction of erythroid progenitors in R-PK deficiency may be useful for the identification of molecular targets of causal treatment.

Acknowledgments

We are indebted to Takako Hamada and Miyuki Yuda for their excellent technical assistance. This work was supported in part by a Grant-in-Aid for Scientific Research from the Japan Society of the Promotion of Science (project nos. 14570131 and 16590254), and also by a Scientific Research Grant from the Ministry of Health, Labor and Welfare (H15-kagaku-002, H18-kagaku-ippan-001), Japan.

References

1. Hirono A, Kanno H, Miwa S, Beutler E. Pyruvate kinase deficiency and other enzymopathies of the erythrocyte. In: Scriver CR, Beaudet AL, Sly WS, Valle D, eds. The Metabolic & Molecular Bases of Inherited Disease. 8th ed. New York: McGraw-Hill; 2001. p. 4637–4664.
2. Takegawa S, Fujii H, Miwa S. Change of pyruvate kinase isozymes from M2- to L-type during development of the RBC. Br J Haematol. 1983;54:467–474.
3. Max-Audit I, Kechemir D, Mitjavila MT, Vainchenker W, Rotten D, Rosa R. Pyruvate kinase synthesis and degradation by normal and pathologic cells during erythroid maturation. Blood. 1988;72: 1039–1044.
4. Tanaka KR, Zerez CR. RBC enzymopathies of the glycolytic pathway. Semin Hematol. 1990;27:165–185.
5. Zanella A, Fermo E, Bianchi P, Valentini G. RBC pyruvate kinase deficiency: molecular and clinical aspects. Br J Haematol. 2005;130: 11–25.
6. Aisaki K, Kanno H, Oyaizu N, Hara Y, Miwa S, Ikawa Y. Apoptotic changes precede mitochondrial dysfunction in red cell-type pyruvate kinase mutant mouse erythroleukemia cell lines. Jpn J Cancer Res. 1999;90:171–179.
7. Morimoto M, Kanno H, Asai H, et al. Pyruvate kinase deficiency of mice associated with nonspherocytic hemolytic anemia and cure of the anemia by marrow transplantation without host irradiation. Blood. 1995;86:4323–4330.
8. Kanno H, Morimoto M, Fujii H, et al. Primary structure of murine red blood cell-type pyruvate kinase (PK) and molecular characterization of PK deficiency identified in the CBA strain. Blood. 1995;86: 3205–3210.
9. Aizawa S, Kohdera U, Hiramoto M, et al. Ineffective erythropoiesis in the spleen of a patient with pyruvate kinase deficiency. Am J Hematol. 2003;74:68–72.
10. Aizawa S, Harada T, Kanbe E, et al. Ineffective erythropoiesis in mutant mice with deficient pyruvate kinase activity. Exp Hematol. 2005; 33:1292–1298.
11. Kanno H, Fujii H, Hirono A, Miwa S. cDNA cloning of human R-type pyruvate kinase and identification of a single amino acid substitution (Thr384→Met) affecting enzymatic stability in a pyruvate kinase variant (PK Tokyo) associated with hereditary hemolytic anemia. Proc Natl Acad Sci U S A. 1991;88:8218–8221.
12. Beutler E, Blume KG, Kaplan JC, Loehr GW, Ramot B, Valentine WN. International Committee for Standardization in Haematology: recommended methods for red cell enzyme analysis. Br J Haematol. 1977;35:331–340.
13. Kanno J, Aisaki K, Igarashi K, et al. "Per cell" normalization method for mRNA measurement by quantitative PCR and microarrays. BMC Genomics. 2006;29:64.
14. Krones A, Jungermann K, Kietzmann T. Cross-talk between the signals hypoxia and glucose at the glucose response element of the L-type pyruvate kinase gene. Endocrinology. 2001;142:2707–2718.
15. Danial NN, Gramm CF, Scorrano L, et al. BAD and glucokinase reside in a mitochondrial complex that integrates glycolysis and apoptosis. Nature. 2003;424:952–956.
16. Shim H, Chun YS, Lewis BC, Dang CV. A unique glucose-dependent apoptotic pathway induced by c-Myc. Proc Natl Acad Sci U S A. 1998;95:1511–1516.
17. Brand K, Netzker R, Aulwurm U, et al. Control of thymocyte proliferation via redox-regulated expression of glycolytic genes. Redox Rep. 2000;5:52–54.
18. Shimizu T, Uehara T, Nomura Y. Possible involvement of pyruvate kinase in acquisition of tolerance to hypoxic stress in glial cells. J Neurochem. 2004;91:167–175.
19. Lee YJ, Kang IJ, Bunger R, Kang YH. Mechanisms of pyruvate inhibition of oxidant-induced apoptosis in human endothelial cells. Microvasc Res. 2003;66:91–101.
20. Basing E, Summer O, Schemer M, Bunger R. Antioxidant pyruvate inhibits cardiac formation of reactive oxygen species through changes in redox state. Am J Physiol Heart Circ Physiol. 2000;279:H2431–H2438.
21. Luzzatto L, Mehta A, Vulliamy T. Glucose 6-phosphate dehydrogenase. In: Scriver CR, Beaudet AL, Sly WS, Valle D, eds. The Metabolic & Molecular Bases of Inherited Disease. 8th ed.. New York: McGraw-Hill; 2001. p. 4517–4554.
22. Neumann CA, Krause DS, Carman CV, et al. Essential role for the peroxiredoxin Prdx1 in erythrocyte antioxidant defense and tumour suppression. Nature. 2003;424:561–565.
23. Lee TH, Kim SU, Yu SL, et al. Peroxiredoxin II is essential for sustaining life span of erythrocytes in mice. Blood. 2003;101:5033–5038.
24. Ferreira P, Morais L, Costa R, et al. Hydrops fetalis associated with erythrocyte pyruvate kinase deficiency. Eur J Pediatr. 2000;159: 481–482.
25. Bowman HS, McKusick VA, Dronamraju KR. Pyruvate kinase deficient hemolytic anemia in an Amish isolate. Am J Hum Genet. 1965;17:1–8.
26. Tanphaichitr VS, Suvatte V, Issaragrisil S, et al. Successful bone marrow transplantation in a child with red blood cell pyruvate kinase deficiency. Bone Marrow Transplant. 2000;26:689–690.

0026-895X/07/7205-1171–1180$20.00
MOLECULAR PHARMACOLOGY
Copyright © 2007 The American Society for Pharmacology and Experimental Therapeutics
Mol Pharmacol 72:1171–1180, 2007

Vol. 72, No. 5
38836/3268509
Printed in U.S.A.

Evaluation of Action Mechanisms of Toxic Chemicals Using JFCR39, a Panel of Human Cancer Cell Lines[S]

Noriyuki Nakatsu, Tomoki Nakamura, Kanami Yamazaki, Soutaro Sadahiro, Hiroyasu Makuuchi, Jun Kanno, and Takao Yamori

Division of Molecular Pharmacology, Cancer Chemotherapy Center, Japanese Foundation for Cancer Research, Koto-ku, Tokyo, Japan (N.N., T.N., K.Y., T.Y.); Division of Cellular and Molecular Toxicology, Biological Safety Research Center, National Institute of Health Sciences, Setagaya-ku, Tokyo, Japan (N.N., J.K.); and Second Department of Surgery, Tokai University School of Medicine, Boseidai, Isehara-City, Kanagawa, Japan (T.N., S.S., H.M.)

Received June 6, 2007; accepted August 16, 2007

ABSTRACT

We previously established a panel of human cancer cell lines, JFCR39, coupled to an anticancer drug activity database; this panel is comparable with the NCI60 panel developed by the National Cancer Institute. The JFCR39 system can be used to predict the molecular targets or evaluate the action mechanisms of the test compounds by comparing their cell growth inhibition profiles (i.e., fingerprints) with those of the standard anticancer drugs using the COMPARE program. In this study, we used this drug activity database-coupled JFCR39 system to evaluate the action mechanisms of various chemical compounds, including toxic chemicals, agricultural chemicals, drugs, and synthetic intermediates. Fingerprints of 130 chemicals were determined and stored in the database. Sixty-nine of 130 chemicals (~60%) satisfied our criteria for the further analysis and were classified by cluster analysis of the fingerprints of these chemicals and several standard anticancer drugs into the following three clusters: 1) anticancer drugs, 2) chemicals that shared similar action mechanisms (for example, ouabain and digoxin), and 3) chemicals whose action mechanisms were unknown. These results suggested that chemicals belonging to a cluster (i.e., a cluster of toxic chemicals, a cluster of anticancer drugs, etc.) shared similar action mechanism. In summary, the JFCR39 system can classify chemicals based on their fingerprints, even when their action mechanisms are unknown, and it is highly probable that the chemicals within a cluster share common action mechanisms.

Determining the action mechanism or identifying the molecular target of a chemical with pharmacological activity or adverse side effects is highly desirable. Although various test methods are currently available for determining the action mechanisms of chemicals, such as methods based on animal models, methods based on cellular models, bacterial mutagenicity test, the uterotropic assay (Kanno et al., 2002), Hershberger test (Hershberger et al., 1953), and the reporter assay for the nuclear receptor agonists, determination of the action mechanisms of pharmacologically active chemicals, including the toxic chemicals, is still a difficult and challenging task. Therefore, it is highly desirable to develop efficient test methods for evaluating toxicity of chemicals.

A number of screening methods are currently available for discovering new anticancer drugs. One very powerful and unique approach using multiple cancer cell lines was developed at NCI (Paull et al., 1989; Weinstein et al., 1992, 1997) and in our laboratory (Yamori et al., 1999; Dan et al., 2002, 2003; Yamori, 2003; Nakatsu et al., 2005; Akashi and Yamori, 2007; Akashi et al., 2007; Nakamura et al., 2007). This bioinformatics-based approach enables mechanism-oriented evaluation of anticancer drugs. For example, we can evaluate the cell toxicity in vitro by determining the 50% growth inhibition (GI50), total growth inhibition, and 50% lethal concentration across a panel of 39 human cancer cell lines (JFCR39). We can also predict the molecular targets or evaluate the action mechanisms of the test compounds by comparing the cell growth inhibition profiles (termed "fingerprints") across the panel for these compounds with those of

This work was supported in part by Grant-in-Aid 17390032 for Scientific Research (B) from Japan Society for the Promotion of Science (to T.Y.); Ministry of Health, Labor, and Welfare Grants-in-Aid H15-kagaku-002, H16-kagaku-003 (to T.Y. and J.K.); Grant-in-Aid 18015049 of the Priority Area "Cancer" from the Ministry of Education, Culture, Sports, Science and Technology of Japan (to T.Y.); and grant 05-13 from National Institute of Biomedical Innovation Japan (to T.Y.)

N. N. and T. N. equally contributed to this study.

Article, publication date, and citation information can be found at http://molpharm.aspetjournals.org.

doi:10.1124/mol.107.038836.

[S] The online version of this article (available at http://molpharm.aspetjournals.org) contains supplemental material.

ABBREVIATIONS: GI50, 50% growth inhibition concentration; GI50, 50% growth inhibition; SN-38, 7-ethyl-10-hydroxycamptothecin; SV-NN, snake venom from *N. nigricollis*; SV-NNK; snake venom from *N. naja kaouthia*.

TABLE 1
List of chemicals tested. Chemical names, abbreviations, and applications/targets/mechanisms of the test compounds are summarized.

JCI No	Name	Abbreviation	Application/Target/Mechanism
−691	Trioctyltin	TOT	Organotin
−690	Triphenyltin	TPT	Organotin
−689	Dibutyltin		Organotin
−688	AM-580		RARα
−687	TTNPB		RAR
−686	13-*cis* Retinoic acid	13-*cis*	RAR
−607	Methoprene		Agricultural chemical
−606	Methoprene acid		RXR
−605	5-aza-2′-deoxycytidine	5-AzaC	Methylation
−604	Carbaryl		Agricultural chemical
−603	Acephate		Agricultural chemical
−602	Sodium arsenite		Agricultural chemical
−601	Testosterone propionate	TP	Testosterone
−600	Ethynyl estradiol	EE	Estrogenic
−599	Thiram		Agricultural chemical
−598	Dimethylformamide	DMF	Solvent
−568	α-Bungarotoxin	αBuTX	Neurotoxin
−567	Snake venom from *Trimeresurus flavoviridis*	SV-TF	Snake venom
−566	Snake venom from *Crotalus atrox*	SV-CA	Snake venom
−565	Snake venom from *Agkistrodon halys blomhoffii*	SV-AHB	Snake venom
−564	Dexamethasone	DEX	Steroid
−563	3-Methylcholanthrene	3-MC	Teratogenicity/carcinogenicity
−562	*N*-Ethyl-*N*-nitrosourea	ENU	Teratogenicity/carcinogenicity
−561	Diethylnitrosamine	DEN	Teratogenicity/carcinogenicity
−560	All *trans*-retinoic acid	ATRA	RAR + RXR
−559	9-cis Retinoic acid	9-cis	RAR
−558	Levothyroxine	T4	Thyroid hormone
−557	3-Amino-1*H*-1,2,4-triazole	3AST	Agricultural chemical
−555	2-Vinylpyridine	2VP	Synthetic intermediate
−553	Phenobarbital	PB	Antiepileptic
−552	Acetaminophen	APAP	Analgetic
−551	Isoniazid		Phthisic
−549	4-Ethylnitrobenzene	4ENB	Synthetic intermediate
−548	1,2-Dichloro-3-nitrobenzene	1,2DC3NB	Pigment/synthetic intermediate
−546	*N*-Methylaniline	NMA	Synthetic intermediate
−545	2-Aminomethylpyridine	2AMP	Synthetic intermediate
−544	1*H*-1,2,4-Triazole		Synthetic intermediate
−543	1*H*-1,2,3-Triazole		Synthetic intermediate
−542	4-Amino-2,6-dichlorophenol	4A2,6DCP	Synthetic intermediate
−541	2,4-Dinitrophenol	2,4 DNP	Agricultural chemical
−513	Capsaicin		Food constituent
−485	2-Methoxyestradiol		Estrogenic
−466	Colcemid		Spindle inhibitor
−465	2,4-Dinitrochlorobenzene	2,4DCB	Pigment/mutagenesis
−464	Troglitazone		Diabetic
−463	Clofibrate		Antilipemic
−459	Bis(2-ethylhexyl)phthalate	DEHP	Plasticizer
−458	Thiourea		Agricultural chemical
−447	Cacodylic acid		Agricultural chemical
−446	Amitrole		Agricultural chemical
−445	4-Octylphenol	OP	Reproductive effector
−444	2,6-Dimethylaniline	2,6-Xylidene	Natural product
−443	1,2-Dibromo-3-chloropropane	DBCP	Agricultural chemical
−442	1,1-Dimethylhydrazine	1,1DMH	Reproductive effector
−441	Sulfanylamide		Agricultural chemical
−440	Streptozotocin		Agricultural chemical
−439	Spironolactone		Aldosterone antagonist
−438	*para*-Aminoazobenzene	pAAB	Pigment/mutagenicity/carcinogenicity
−437	*para*-Cresidine		Pigment/carcinogenicity
−436	Neostigmine bromide		Parasympathomimetics
−435	*para*-Dichlorobenzene	pDCB	Pigment/Agricultural chemical
−434	Phenytoin		Antiepileptic
−433	*ortho*-Toluidine	oToluidine	Pigment
−432	Imipramine		Antidepressant
−431	Cobalt chloride		Teratogenicity/mutagenicity
−428	Atrazine		Agricultural chemical
−427	Propylthiouracil		Teratogenicity/carcinogenicity
−426	Thalidomide (L + D)		Teratogenicity
−425	Carbon tetrachloride	CCl_4	Teratogenicity/carcinogenicity
−424	Hydroquinone		Oxidative stress
−423	Monocrotaline		Mutagenicity/carcinogenicity
−422	Vinyl chloride		Carcinogenicity
−421	Tributyltin chloride	TBT	Ship bottom paint/organotin
−420	Valproic acid		Antiepileptic
−419	Benzene		Carcinogenicity

TABLE 1—(*Continued*)

JCI No	Name	Abbreviation	Application/Target/Mechanism
−418	Acrylamide		Neurotoxin/carcinogenicity
−417	Hexachlorobenzene	BHC	Agricultural chemical/carcinogenicity
−346	2-Deoxyglucose	2-DG	Glycolytic pathway/glycosylation inhibitor
−325	Pentachlorophenol	PCP	Agricultural chemical/teratogenicity/carcinogenicity
−324	Aniline		Oxidative stress/methemoglobinemia/carcinogenicity
−323	Triazine		Agricultural chemical
−322	Edifenphos	EDDP	Agricultural chemical/antibiotics/choline esterase
−321	γ-1,2,3,4,5,6-Hexachlorocyclohexane	γ-BHC	Agricultural chemical/carcinogenicity
−320	Dichlorvos	DDVP	Agricultural chemical/teratogenicity/carcinogenicity
−319	*O*-Ethyl *O*-4-nitrophenyl phenylphosphonothioate	EPN	Agricultural chemical
−318	Cadmium chloride	$CdCl_2$	Teratogenicity/carcinogenicity
−317	Phenylmercury acetate	PMA	Fungicides/mutagenicity
−316	Mercaptoacetic acid		Synthetic intermediate
−315	1,3-Diphenylguanidine	DPG	Vulcanizing agent
−314	3,4,4′-Trichlorocarbanilide	TCC	Cosmetics/antibacterial agent
−313	3-Iodo-2-propynyl butylcarbamate	IPBC	Antibacterial agent
−311	2,3,3,3−2′,3′,3′,3′-Octachlorodipropylether	S-421	Agricultural chemical/antibacterial agent
−310	1,2-Benzisothiazolin-3-one	BIT	Antibacterial agent
−309	Isobornylthiocyanoacetate	IBTA	Antibacterial agent
−308	*p*-Chlorophenyl-3-iodopropargylformal	CPIP	Antibacterial agent
−307	Zinc butylxanthate	ZBX	Vulcanizing agent
−306	Polypropylene glycol	PG	Synthetic intermediate
−305	10,10′-Oxy-bis(phenoxyarsine)	OBPA	Antibacterial agent
−296	Snake venom from *Naja naja kaouthia*	SV-NNK	Snake venom
−295	Snake venom from *Naja nigricollis*	SV-NN	Snake venom
−294	2,5-di(*tert*-butyl)-1,4-Hydroquinone	DTBHQ	Oxidative stress
−293	Ibotenic Acid		Mushroom toxin/neurotoxin
−292	*N*-Methy-4-phenyl-1,2,3,6-tetrahydropyridine	MPTP	Neurotoxin
−289	Tetrodotoxin		Natural product/Na^+ channel inhibitor
−288	ICI 182,780		Estrogen antagonist
−275	Benzophenone		Agricultural chemical
−274	1,2-Dibromo-3-chloropropane	DBCP	Antibacterial agent/insecticide/carcinogenicity
−273	Zineb		Agricultural chemical
−272	Dieldrin		Insecticide
−271	Hexachlorobenzene	HCB	Antibacterial agent/carcinogenicity
−270	Ziram		Antibacterial agent/vulcanizing agent
−269	Chlordane		Insecticide/carcinogenicity
−268	4,4′-Dichlorodiphenyltrichloroethane	p,p′-DDT	Insecticide/carcinogenicity/teratogenicity
−267	Bisphenol A	BPA	Estrogenic
−266	17-β-Estradiol	E2	Estrogenic
−265	Diethylstilbestrol	DES	Estrogenic
−261	Paraquat		Agricultural chemical/oxidative stress
−247	Ouabain		Cardiac glycosides
−245	Okadaic acid		Natural product/PP1, PP2A inhibitor
−242	Antimycin A1		Agricultural chemical
−232	Digoxin		Cardiac glycosides
−201	OH-Flutamide		Flutamide derivative/androgen antagonist
−200	Flutamide		Anticancer drugs/androgen antagonist
−185	30% H_2O_2		Oxidative stress
−182	*N*-Acetyl-L-cysteine	NAC	Super oxyside scavenger
−181	L-Ascorbic acid		Food constituent
−179	Dopamine		Neurotransmitter
−177	Caffeine		Food constituent
−168	Cycloheximide		Protein synthesis inhibitor
−144	4-Hydroxyphenylretinamide	4-HPR	RAR
−137	Indomethacin		COX inhibitor
−99	SN-38		Irinotecan derivative/Topo I
−96	Toremifene		Anticancer drugs/estrogen antagonist
−95	Tamoxifen		Anticancer drugs/estrogen antagonist
−63	Cyclosporin A		Anticancer drugs/helper T cell
−46	HCFU		Anticancer drugs/antimetabolite(pyrimidine)
−36	Docetaxel		Anticancer drugs/tubulin
−35	Paclitaxel		Anticancer drugs/tubulin
−34	Colchicine		Antipodagric/tubulin
−33	Cisplatin		Anticancer drugs/DNA cross linker
−32	Carboplatin		Anticancer drugs/DNA cross linker
−31	Irinotecan		Anticancer drugs/Topo I
−30	Camptothecin	CPT	Anticancer drugs/Topo I
−24	Methotrexate		Anticancer drugs/DHFR
−19	Vincristine		Anticancer drugs/tubulin
−18	Vinblastine		Anticancer drugs/tubulin
−16	Mitomycin-C	MMC	Anticancer drugs/DNA alkylator
−9	Tegafur		Anticancer drugs/antimetabolite(pyrimidine)
−8	5-Fluorouracil	5-FU	Anticancer drugs/antimetabolite(pyrimidine)
−5	Cytarabine		Anticancer drugs/antimetabolite(pyrimidine)
−4	Nitrogen mustard		Anticancer drugs/DNA alkylator

RAR, retinoic acid receptor; RXR; retinoid X receptor.

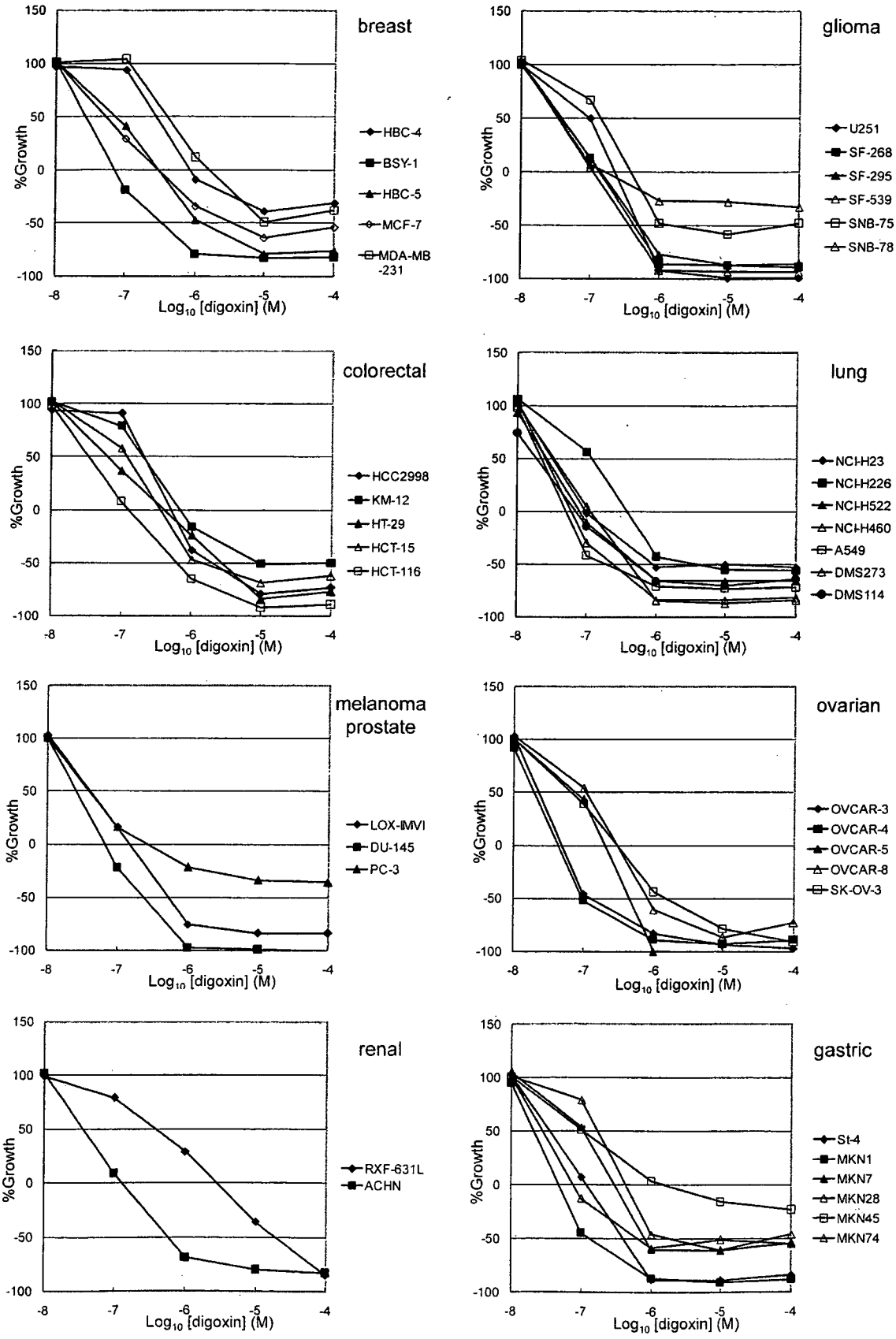

Fig. 1. Dose response curves of digoxin against growth of JFCR-39 cells. The *x*-axis represents concentration of digoxin and the *y-axis* represents percentage growth. The GI50 represents the concentration required to inhibit cell growth by 50% compared with untreated controls.

the standard anticancer drugs using the COMPARE algorithm (Yamori et al., 1999). We have used this system successfully and demonstrated that the molecular targets of the novel chemicals MS-274, FJ5002, and ZSTK474 were topoisomerases I and II (Yamori et al., 1999), telomerase (Naasani et al., 1999), and phosphatidylinositol 3-kinase (Yaguchi et al., 2006), respectively. Several other interesting studies, based on a panel of cancer cells, classified anticancer drugs according to their action mechanisms or molecular targets by cluster analysis of their GI50 values (Weinstein et al., 1992, 1997; Dan et al., 2002). Correlation analysis has also been used to explore the genes associated with the sensitivity of the cells in the panel to anticancer drugs (Scherf et al., 2000; Okutsu et al., 2002; Zembutsu et al., 2002; Nakatsu et al., 2005).

In this study, we have examined the potential of the JFCR39 system in classifying various chemicals, and predicted their action mechanisms. For this purpose, we have determined the fingerprints of 130 different types of chemicals including toxic chemicals, pesticides, drugs and synthetic intermediates, and then classified these chemicals according to the cluster analysis of their fingerprints.

Materials and Methods

Cell Lines and Cell Cultures. The panel of human cancer cell lines has been described previously (Yamori et al., 1999; Dan et al., 2002) and consists of the following 39 human cancer cell lines: lung cancer, NCI-H23, NCI-H226, NCI-H522, NCI-H460, A549, DMS273, and DMS114; colorectal cancer, HCC-2998, KM-12, HT-29, HCT-15, and HCT-116; gastric cancer, MKN-1, MKN-7, MKN-28, MKN-45, MKN-74, and St-4; ovarian cancer, OVCAR-3, OVCAR-4, OVCAR-5, OVCAR-8, and SK-OV-3; breast cancer, BSY-1, HBC-4, HBC-5, MDA-MB-231, and MCF-7; renal cancer, RXF-631L and ACHN; melanoma, LOX-IMVI; glioma, U251, SF-295, SF-539, SF-268, SNB-75, and SNB-78; and prostate cancer, DU-145 and PC-3. All cell lines were cultured in RPMI 1640 medium (Nissui Pharmaceutical, Tokyo, Japan) with 5% fetal bovine serum, penicillin (100 units/ml), and streptomycin (100 μg/ml) at 37°C under 5% CO_2.

Determination of Cell Growth Inhibition Profiles. Growth inhibition experiments were performed to assess the sensitivity of the cells to various chemicals as described before (Yamori et al., 1999; Dan et al., 2002). Growth inhibition was measured by determining the changes in the amounts of total cellular protein after 48 h of chemical treatment using a sulforhodamine B assay. For each chemical, the growth assay was performed using a total of five different concentrations of the chemical (for example, 10^{-4}, 10^{-5},

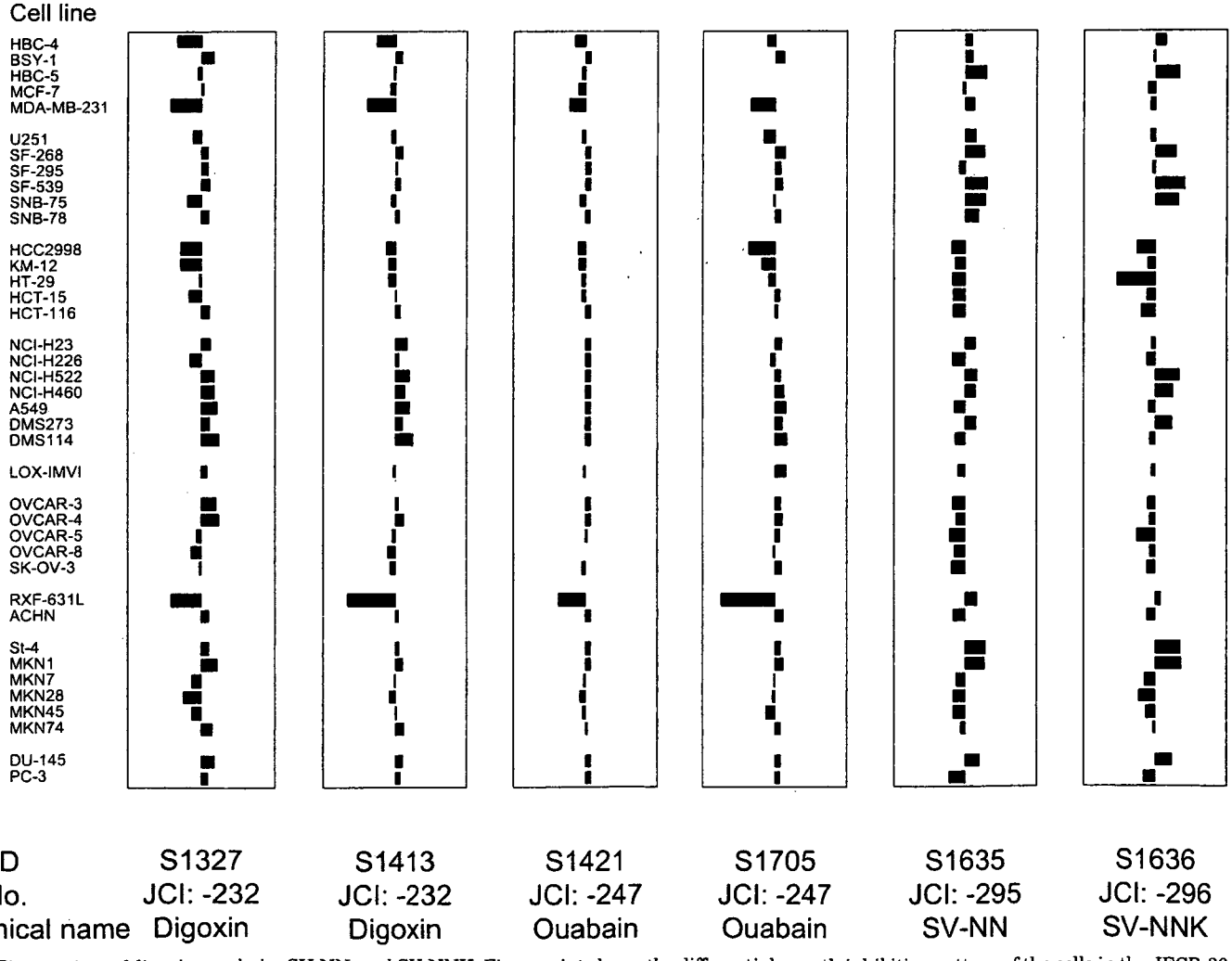

Fig. 2. Fingerprints of digoxin, ouabain, SV-NN, and SV-NNK. Fingerprint shows the differential growth inhibition pattern of the cells in the JFCR-39 panel against the test chemical. The *X*-axis represents relative value of GI50; $(-1) \times (\log GI50 - MG\text{-}MID)$; MG-MID is the mean value of the log GI50. Zero means the mean GI50 and one means the GI50 value is 10-fold more sensitive than the mean GI50. Exp-ID and JCI numbers are the ID for the experiment and ID for the chemical, respectively, in our database.

10^{-6}, 10^{-7}, and 10^{-8} M) and one negative control. All assays were performed in duplicate. This GI50 calculation method is well established and reliable through anticancer drug screen using NCI60 as well as JFCR39 (Paull et al., 1989; Yamori et al., 1999; Yamori, 2003). At each test concentration, the percentage growth was calculated using the following seven absorbance measurements: growth at time 0 (T0), growth of the control cells (C), and test growth in the presence of five different concentrations (T) of a drug. The percentage growth inhibition was calculated as: % growth = 100 × [(T − T0)/(C − T0)] when T ≥ T0, and % growth = 100 × [(T − T0)/T] when T < T0. The GI50 values, which represent 50% growth inhibition concentration, were calculated as 100 × [(T − T0)/(C − T0)] = 50. When the GI50 of a chemical could not be calculated, the highest used concentration was assigned as its GI50 value. Absolute values of GI50 were then log transformed for further analysis. We certified the accuracy of measured GI50 data by using reference control chemicals, such as mitomycin-C, paclitaxel, and SN-38, in every experiment and by checking the dose response curves.

Chemicals. Spironolactone, *para*-aminoazobenzene, *para*-cresidine, neostigmine bromide, *para*-dichlorobenzene, phenytoin, *ortho*-toluidine, imipramine, cobalt chloride, atrazine, propylthiouracil, (D,L)-thalidomide, carbon tetrachloride, hydroquinone, monocrotaline, vinyl chloride, tributyl-tin chloride, valproic acid, benzene, acrylamide, pentachlorophenol, aniline, 1,3-diphenylguanidine, polypropylene glycol, 10,10′-oxy-bis(phenoxyarsine), testosterone propionate, carbaryl, acephate, bisphenol A, 17-β-estradiol, diethylstilbestrol, and α-bungarotoxin were purchased from Wako (Tokyo, Japan). Snake venoms from *Agkistrodon halys blomhoffii*, *Trimeresurus flavoviridis*, *Crotalus atrox*, *Naja nigricollis*, and *Naja naja kaouthia* were purchased from Latoxan (Valence, France). 2-Aminomethylpyridine, 1*H*-1,2,4-triazole, 1*H*-1,2,3-triazole, 3,4,4′-trichlorocarbanilide, edifenphos, dichlorvos, *O*-ethyl *O*-4-nitrophenyl phenylphosphonothioate, 2,4-dinitrophenol, *N*-methylaniline, 1,2-dichloro-3-nitrobenzene, 4-ethylnitrobenzene, 2-vinylpyridine, 3-amino-1*H*-1,2,4-triazole, *N*-ethyl-*N*-nitrosourea, 5-aza-2′-deoxycytidine, ethynyl estradiol, 3-methylcholanthrene, phenobarbital, acetaminophen, isoniazid, capsaicin, *N*-deacetyl-*N*-methylcolchicine (Colcemid), 2.4-dinitrochlorobenzene, and dexamethasone were from Sigma Chemicals (St. Louis, MO). Methoprene acid, methoprene, all-*trans* retinoic acid, and 9-cis retinoic acid were from BIOMOL International L.P. (Plymouth Meeting, PA). Levothyroxine was from MP Biomedicals (Irvine, CA). 3-Iodo-2-propynyl butylcarbamate was from Olin Japan Inc. (Tokyo, Japan), *p*-chlorophenyl-3-iodopropargylformal was from Nagase ChemteX (Osaka, Japan), and 2,3,3,3–2′,3′,3′,3′-octachlorodipropylether was from Sankyo Chemical Industries, Ltd. (Tokyo, Japan). 1,2-Benzisothiazolin-3-one was from Riverson (Osaka, Japan), zinc butylxanthate was from Ouchishinko Chemical Industrial Co., Ltd. (Tokyo, Japan), and 4-amino-2,6-dichlorophenol was from Tokyo Kasei Kogyo Co. Ltd. (Tokyo, Japan).

Hierarchical Clustering. Hierarchical clustering analysis was carried out using the average linkage method and the "GeneSpring" software (Silicon Genetics, Inc., Redwood, CA). Pearson correlation coefficients were used to determine the degree of similarity.

Results

Sensitivity of JFCR39 to Chemicals. Sensitivity of the JFCR39 panel of cells to 130 chemicals was determined as described under *Materials and Methods*. Table 1 summarizes

TABLE 2

Log_{10} GI50 values of chemicals for each cell line in the JFCR-39 panel

Hi-conc means the highest concentration of the test chemical used. When the growth inhibition was over 50% at the Hi-Conc, GI_{50} was assigned the Hi-Conc value.

Exp-ID	S3416	S3415	S3413	S3245	S3117	S3414	S3118	S3246	S3125	S3124	S3123	S1636	S1635	S1634	S1718
JCI No	−687	−686	−559	−559	−559	−560	−560	−560	−567	−566	−565	−296	−295	−294	−294
Name or Abbr.	TTNPB	13-*cis*	9-*cis*			ATRA			SV-TF	SV-CA	SV-AHB	SV-NNK	SV-NN	DTBHQ	
Hi-Conc.	−4	−4	−4	−4	−4	−4	−4	−4	−4	−4	−4	−4	−4	−4	−4
HBC-4	−4.76	−4.00	−4.53	−4.40	−4.43	−4.42	−4.41	−4.41	−5.87	−5.80	−5.66	−7.25	−7.31	−4.72	−4.80
BSY-1	−4.78	−4.16	−4.60	−4.73	−4.73	−4.69	−4.70	−4.81	−6.31	−6.06	−5.76	−6.93	−7.34	−5.07	−4.93
HBC-5	−4.80	−4.41	−4.56	−4.57	−4.61	−4.61	−4.47	−4.51	−6.98	−6.45	−5.73	−7.64	−7.72	−4.89	−4.78
MCF-7	−4.73	−4.35	−4.40	−4.39	−4.48	−4.48	−4.54	−4.66	−5.87	−5.78	−5.68	−6.77	−7.08	−5.29	−5.25
MDA-MB-231	−4.75	−4.21	−4.70	−4.55	−4.69	−4.63	−4.53	−4.65	−5.90	−5.86	−5.84	−6.84	−7.39	−5.52	−5.30
U251	−4.77	−4.14	−4.61	−4.51	−4.61	−4.57	−4.45	−4.63	−6.45	−5.76	−5.70	−6.85	−7.44	−4.96	−5.11
SF-268	−4.75	−4.00	−4.24	−4.55	−4.40	−4.47	−4.48	−4.76	−5.90	−5.79	−5.70	−7.53	−7.67	−4.77	−4.81
SF-295	−4.80	−4.29	−4.54	−4.66	−4.60	−4.59	−4.48	−4.57	−6.19	−5.80	−5.74	−6.89	−6.97	−4.87	−4.97
SF-539	−4.95	−4.35	−4.75	−4.80	−4.79	−4.80	−4.71	−4.76	−6.39	−5.96	−5.81	−7.79	−7.75	−4.79	−4.86
SNB-75	−5.31	−5.28	−5.13	−5.19		−4.71	−4.69	−4.87	−6.41	−6.33	−5.93	−7.60	−7.70	−4.67	−4.80
SNB-78	−4.77	−4.25	−4.69	−4.78	−4.86	−4.49	−4.70	−4.68	−6.19	−6.00	−5.95	−6.97	−7.53	−4.75	−4.75
HCC2998	−4.68	−4.00	−4.48	−4.61	−4.62	−4.55	−4.62	−4.76	−5.91	−5.75	−5.67	−6.47	−6.77	−4.82	−4.75
KM-12	−4.70	−4.00	−4.46	−4.51	−4.48	−4.51	−4.47	−4.58	−5.93	−5.80	−5.65	−6.77	−6.87	−4.74	−4.77
HT-29	−4.73	−4.00	−4.47	−4.53	−4.50	−4.60	−4.52	−4.56	−5.90	−5.80	−5.56	−5.89	−6.78	−4.80	−4.89
HCT-15	−4.72	−4.25	−4.45	−4.49	−4.48	−4.52	−4.57	−4.53	−5.88	−5.76	−5.57	−6.73	−6.82	−4.72	−4.77
HCT-116	−4.77	−4.07	−4.67	−4.59	−4.67	−4.71	−4.61	−4.64	−6.46	−6.10	−5.77	−6.58	−6.82	−4.98	−5.13
NCI-H23	−4.74	−4.00	−4.47	−4.60	−4.59	−4.61	−4.55	−4.63	−6.11	−5.75	−5.72	−6.86	−7.42	−4.76	−4.90
NCI-H226	−4.72	−4.00	−4.61	−4.68	−4.78	−4.80	−4.54	−5.48	−5.95	−5.81	−5.76	−6.73	−6.78	−4.89	−4.91
NCI-H522	−4.72	−4.45	−4.68	−4.82	−4.77	−4.71	−4.71	−4.68	−6.45	−5.99	−5.78	−7.62	−7.46	−5.37	−5.37
NCI-H460	−4.70	−4.00	−4.55	−4.63	−4.58	−4.68	−4.55	−4.49	−5.96	−5.82	−5.72	−7.44	−7.42	−4.84	−4.84
A549	−4.79	−4.00	−4.72	−4.77	−4.78	−4.70	−4.62	−4.53	−5.91	−5.79	−5.71	−6.80	−6.83	−4.83	−4.87
DMS273	−4.57	−4.21	−4.50	−4.62	−4.55	−4.57	−4.51	−4.49	−6.20	−5.81	−5.72	−7.43	−7.44	−4.91	−4.98
DMS114	−4.77	−4.16	−4.33	−4.62	−4.49	−4.51	−4.53	−4.61	−6.66	−6.33	−5.77	−6.83	−6.88	−5.12	−5.21
LOX-IMVI	−4.77	−4.69	−4.68	−4.66	−4.70	−4.77	−4.74	−4.74	−6.75	−6.59	−5.76	−6.86	−6.94	−5.05	−5.15
OVCAR-3	−4.77	−4.38	−4.56	−4.67	−4.72	−4.64	−4.62	−4.71	−6.61	−6.13	−5.89	−6.77	−6.79	−4.89	−4.86
OVCAR-4	−4.72	−4.05	−4.63	−4.64	−4.64	−4.58	−4.39	−4.54	−6.73	−6.23	−5.80	−6.82	−6.90	−5.13	−4.90
OVCAR-5	−4.75	−4.00	−4.33	−4.39	−4.42	−4.44	−4.34	−4.44	−5.92	−5.74	−5.67	−6.46	−6.71	−5.22	−5.26
OVCAR-8	−4.75	−4.23	−4.50	−4.53	−4.59	−4.66	−4.67	−4.70	−5.95	−5.77	−5.69	−6.82	−6.84	−4.64	−4.70
SK-OV-3	−4.79	−4.00	−4.49	−4.51	−4.81	−4.52	−4.54	−4.50	−5.76	−5.64	−4.91	−6.75	−6.76	−4.64	−4.74
RXF-631L	−4.77	−4.00	−4.54	−4.58	−4.60	−4.72	−4.63	−4.61	−5.91	−5.80	−5.59	−7.13	−7.46	−4.81	−4.84
ACHN	−4.73	−4.00	−4.56	−4.66	−4.56	−4.50	−4.40	−4.76	−5.90	−5.79	−5.73	−6.74	−6.80	−4.71	−4.83
St-4	−4.74	−4.00	−4.42	−4.54	−4.65	−4.53	−4.49	−4.57	−5.91	−5.81	−5.76	−7.65	−7.70	−4.68	−4.75
MKN1	−4.75	−4.33	−4.56	−4.63	−4.62	−4.56	−4.45	−4.48	−6.15	−5.81	−5.78	−7.67	−7.68	−4.59	−4.81
MKN7	−4.78	−4.40	−4.68	−4.59	−4.70	−4.73	−4.56	−4.65	−6.29	−5.85	−5.76	−6.70	−6.90	−4.79	−4.84
MKN28	−4.71	−4.28	−4.56	−4.59	−4.59	−4.65	−4.56	−4.60	−6.10	−5.93	−5.68	−6.51	−6.81	−4.72	−4.89
MKN45	−4.72	−4.00	−4.51	−4.41	−4.46	−4.73	−4.41	−4.43	−6.06	−5.90	−5.69	−6.71	−6.82	−4.71	−4.87
MKN74	−4.74	−4.40	−4.61	−4.63	−4.61	−4.73	−4.68	−4.67	−5.97	−5.92	−5.61	−6.92	−7.00	−5.10	−5.42
DU-145	−4.68	−4.00	−4.25	−4.78	−4.41	−4.42	−4.44	−4.54	−6.08	−5.82	−5.75	−7.43	−7.55	−4.59	−5.02
PC-3	−4.74	−4.00	−4.58	−4.65	−4.48	−4.74	−4.39	−4.51	−5.83	−5.77	−5.61	−6.67	−6.69	−4.89	−4.74

abbreviations, applications, targets, and known mechanisms of 130 chemicals and 21 anticancer drugs. Approximately 15% of the chemicals were assessed twice or more. Approximately 40% of the chemicals tested had little effect on the growth of cells in the JFCR39 panel. However, the rest of the chemicals significantly inhibited the cell growth across the JFCR39 panel. For example, Fig. 1 shows the dose response curves of the cells in the JFCR39 panel against digoxin. The concentration at which the cell growth is inhibited by 50% represents GI50. Figure 2 shows the fingerprints of four chemicals [digoxin, ouabain, snake venom from *N. nigricollis* (SV-NN), and snake venom from *N. naja kaouthia* (SV-NNK)], which differentially inhibited the growth of cells in the JFCR39 panel; these fingerprints were drawn based on a calculation using a set of GI50s and clearly represented the GI50 pattern. These results were highly reproducible in that the Pearson correlation coefficient of the duplicate experiments for digoxin was 0.839 ($p < 0.001$) and that for ouabain was 0.864 ($p < 0.001$). It is noteworthy that, digoxin and ouabain, both of which are cardiac glycosides and inhibit Na-K ATPase, showed similar fingerprints. The fingerprints of SV-NNK and SV-NN, which belong to the elapidae, known as cobras, were also similar, but were different from the fingerprints of digoxin and ouabain. Table 2 summarizes only a portion of the GI50 values from 160 experiments involving 130 chemicals and 42 experiments involving 21 anticancer drugs. GI50 values from all experiments are described in the Supplemental Data (Table S1). All these data were stored in a chemosensitivity database and used for further analysis.

Classification of the Chemicals by Hierarchical Clustering. Sixty-nine chemicals were selected for further analysis based on the following criteria: 1) GI50 values for the test chemical can be determined for at least 10 cell lines in the JFCR39 panel, and 2) the range of log GI50 for the test chemical is more than 0.6, suggesting differential growth inhibition. We analyzed the GI50 values of these 69 chemicals and 20 anticancer drugs by hierarchical clustering analysis (Fig. 3). We found approximately 12 clusters (threshold: $r = 0$, Fig. 3, clusters A–L), which were further divided into 49 subclusters (threshold: $r = 0.408$, Fig. 3, clusters A1–L6).

Analysis of Clusters. Most anticancer drugs we have tested belonged either to cluster A or cluster H, depending on their modes of action (Dan et al., 2002). The targets of the anticancer drugs belonging to the cluster A were related to DNA (Topo I, antimetabolite of pyridine, DNA alkylator) and the target of the anticancer drugs belonging to the cluster H was tubulin. We presently found that cisplatin exceptionally belonged to cluster F2, not cluster A, although it is known to cross-link DNA strands (Jamieson and Lippard, 1999; Wong and Giandomenico, 1999). We were also able to precisely group the clusters into several subclusters having similar characteristics. For example, the cardiac glycosides digoxin and ouabain were grouped in one cluster (cluster F3). SV-

S3243	S3244	S1534	S3237	S3238	S1525	S3236	S1928	S1421	S1705	S1327	S1413	S1413	S3408	S3409	S2421
−599	−599	−270	−270	−270	−261	−261	−261	−247	−247	−232	−232	−232	−421	−421	−421
Thiram		Ziram			Paraquat			Ouabain		Digoxin			TBT		
−4	−4	−4	−4	−4	−4	−3	−4	−4	−6	−4	−4	−4	−4	−4	−4
−4.71	−4.79	−5.80	−5.73	−5.70	−4.00	−3.61	−4.00	−7.54	−7.28	−6.57	−6.96	−6.96	−6.79	−6.77	−6.72
−6.97	−7.12	−6.85	−6.76	−6.60	−4.00	−4.45	−4.51	−8.00	−7.76	−7.58	−7.68	−7.68	−7.03	−7.01	−6.83
−7.41	−7.66	−7.18	−7.47	−7.47	−4.68	−4.70		−7.76	−7.51	−7.15	−7.44	−7.44	−6.76	−6.88	−6.83
−4.77	−4.80	−6.00	−5.84	−5.83	−4.06	−3.72	−4.00	−7.64	−7.51	−7.29	−7.39	−7.39	−6.86	−6.84	−6.79
−4.66	−4.68	−5.64	−5.75	−5.63	−4.00	−3.57	−4.00	−7.40	−6.81	−6.41	−6.72	−6.72	−6.83	−6.81	−6.70
−4.75	−4.78	−5.71	−5.79	−5.82	−4.00	−3.69	−4.00	−7.75	−7.16	−7.01	−7.40	−7.40	−6.79	−6.77	−6.72
−4.86	−4.96	−5.74	−5.83	−7.01	−4.00	−4.08	−4.00	−8.00	−7.77	−7.42	−7.70	−7.70	−6.84	−6.85	−6.71
−4.77	−4.89	−5.71	−5.70	−5.79	−4.47	−4.37	−4.20	−8.00	−7.64	−7.42	−7.55	−7.55	−6.75	−6.73	−6.76
−4.75	−4.88	−5.73	−5.75	−5.77	−4.00	−4.03	−4.00	−8.00	−7.70	−7.46	−7.63	−7.63	−6.77	−6.72	−6.67
−4.71	−4.96	−5.79	−5.92	−5.80	−4.00	−3.94	−4.00	−7.70	−7.45	−6.86	−7.40	−7.40	−6.99	−6.95	−7.05
−4.70	−4.78	−5.69	−5.64	−5.69	−4.00	−3.78	−4.00	−7.98	−7.64	−7.45	−7.60	−7.60	−6.72	−6.79	−6.70
−4.82	−4.69	−5.76	−5.79	−5.81	−4.00	−3.70	−4.00	−7.64	−6.77	−6.68	−7.25	−7.25	−6.77	−6.79	−6.72
−4.80	−4.80	−5.43	−5.74	−5.73	−4.00	−3.58	−4.00	−7.67	−7.12	−6.69	−7.34	−7.34	−7.00	−6.98	−6.74
−4.68	−4.85	−5.75	−5.77	−5.76	−4.10	−4.03	−4.07	−7.75	−7.31	−7.20	−7.34	−7.34	−6.89	−6.84	−6.66
−4.68	−4.75	−5.70	−5.72	−5.83	−4.00	−3.64	−4.00	−7.74	−7.63	−6.92	−7.54	−7.54	−6.88	−6.84	−6.70
−4.72	−4.72	−5.74	−5.68	−5.77	−4.00	−3.60	−4.00	−8.00	−7.57	−7.47	−7.62	−7.62	−6.90	−6.85	−6.74
−4.69	−4.78	−5.96	−5.85	−5.84	−4.19	−4.18	−4.00	−8.00	−7.67	−7.50	−7.84	−7.84	−6.90	−6.85	−6.76
−6.33	−6.74	−5.63	−5.96	−6.12	−4.41	−4.41	−4.00	−8.00	−7.37	−6.93	−7.61	−7.61	−6.99	−6.91	−6.74
−7.49	−7.50	−7.44	−7.66	−8.00	−4.49	−4.71	−4.59	−8.00	−7.64	−7.59	−7.91	−7.91	−6.83	−6.80	−6.25
−6.14	−6.16	−6.30	−6.10	−6.15	−4.30	−4.45	−4.37	−8.00	−7.74	−7.60	−7.77	−7.77	−6.98	−6.98	−6.56
−4.84	−4.82	−5.97	−5.91	−5.91	−4.49	−4.49	−4.41	−8.00	−7.80	−7.66	−7.91	−7.91	−6.82	−6.87	−6.73
−6.64	−6.58	−6.43	−6.84	−6.82	−4.25	−4.43	−4.30	−8.00	−7.71	−7.48	−7.72	−7.72	−6.74	−6.75	−6.70
−7.18	−7.39	−7.37	−7.38	−7.43	−4.50	−4.63	−4.27	−8.00	−7.84	−7.73	−8.00	−8.00	−7.11	−7.12	−7.02
−4.68	−4.71	−5.66	−5.71	−5.70	−4.00	−3.51	−4.00	−7.80	−7.80	−7.39	−7.46	−7.46	−6.93	−6.94	−6.76
−4.86	−6.25	−6.07	−6.35	−6.32	−4.00	−4.46	−4.28	−8.00	−7.66	−7.64	−7.59	−7.59	−6.80	−6.82	−6.74
−4.77	−6.67	−5.90	−5.91	−5.87	−4.00	−4.21	−4.48	−8.00	−7.71	−7.71	−7.72	−7.72	−6.91	−7.20	−6.80
−4.90	−6.00	−6.11	−6.91	−6.74	−4.00	−3.98	−4.00	−7.89	−7.62	−7.12	−7.42	−7.42	−6.90	−6.93	−6.75
−4.62	−4.74	−5.59	−5.68	−5.67	−4.00	−3.84	−4.00	−7.85	−7.44	−6.97	−7.29	−7.29	−6.73	−6.67	−6.57
−4.39	−4.38	−4.92	−5.49	−5.53	−4.00	−3.39	−4.00	−7.74	−7.67	−7.18	−7.38	−7.38	−6.80	−6.77	−6.68
−4.75	−4.65	−5.57	−5.63	−5.60	−4.00	−3.60	−4.00	−7.10	−6.00	−6.42	−6.20	−6.20	−6.78	−6.76	−6.68
−4.52	−4.60	−5.64	−5.68	−5.69	−4.00	−3.51	−4.00	−8.00	−7.72	−7.44	−7.59	−7.59	−6.78	−6.77	−6.76
−4.59	−4.72	−5.99	−5.73	−5.81	−4.00	−3.58	−4.00	−8.00	−7.65	−7.45	−7.60	−7.60	−6.80	−6.80	−6.72
−4.80	−4.85	−6.82	−5.84	−5.92	−4.41	−4.61	−4.48	−8.00	−7.72	−7.68	−7.72	−7.72	−7.25	−7.15	−6.87
−4.79	−4.82	−6.56	−5.84	−5.82	−4.08	−4.29	−4.32	−7.80	−7.48	−6.98	−7.47	−7.47	−7.34	−7.07	−6.86
−7.18	−7.21	−5.82	−7.09	−7.13	−4.00	−4.40	−4.18	−7.70	−7.42	−6.77	−7.37	−7.37	−6.84	−6.82	−6.87
−6.65	−6.71	−6.05	−7.18	−6.86	−4.00	−4.29	−4.35	−7.77	−7.25	−6.99	−7.52	−7.52	−6.96	−6.97	−6.87
−7.05	−7.08	−6.35	−5.86	−7.05	−4.00	−4.47	−4.06	−7.91	−7.65	−7.55	−7.74	−7.74	−6.97	−7.37	−7.05
−4.47	−4.70	−5.68	−5.68	−5.65	−4.00	−3.57	−4.00	−8.00	−7.64	−7.59	−7.71	−7.71	−6.90	−6.89	−6.70
−4.42	−4.77	−5.61	−5.53	−5.56	−4.00	−3.64	−4.37	−8.00	−7.62	−7.41	−7.62	−7.62	−6.77	−6.78	−6.73

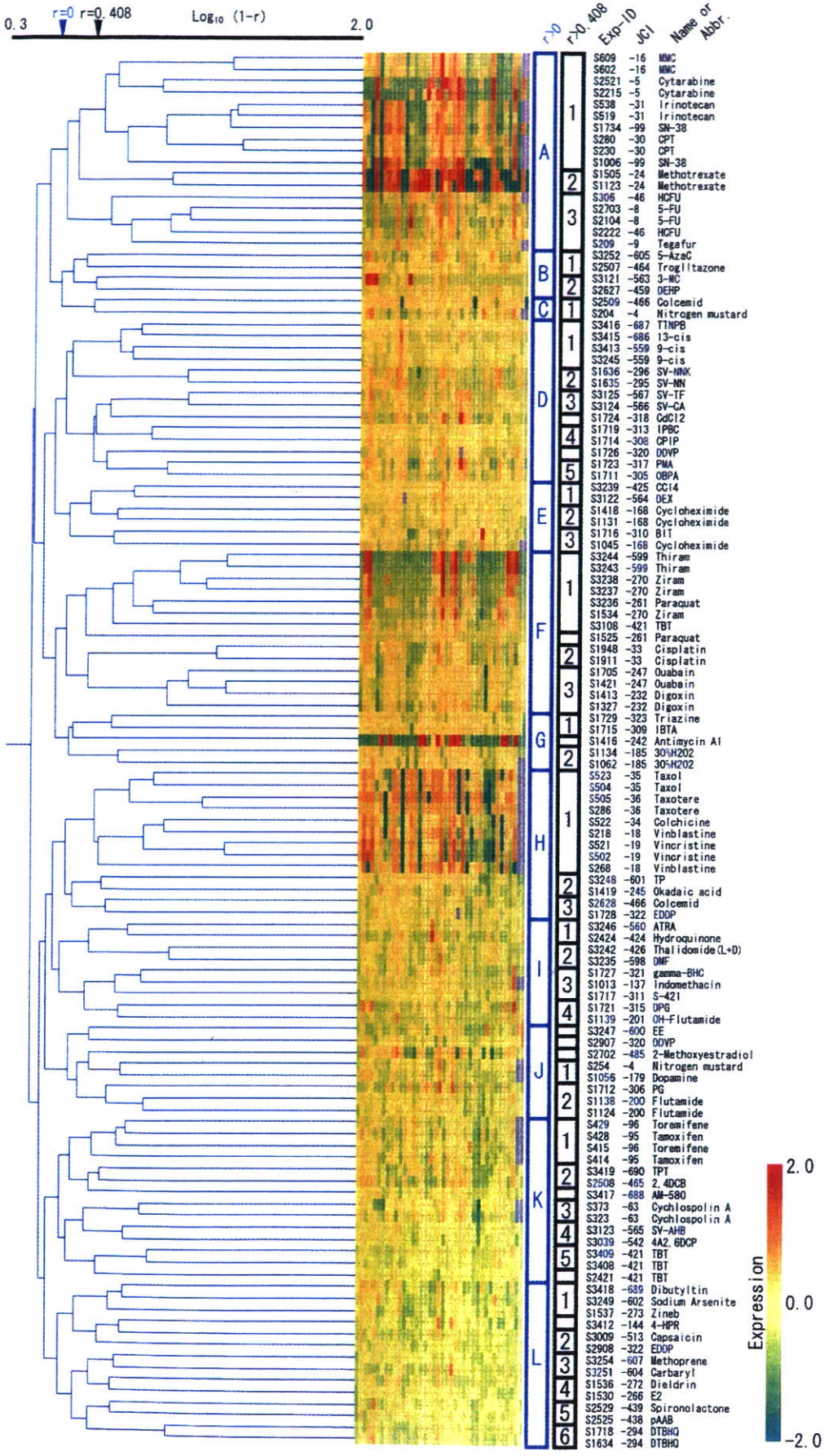

Fig. 3. Hierarchical clustering of 69 test chemicals and 20 anticancer drugs based on their GI50 values. Hierarchical clustering method was an "average linkage method" using the Pearson correlation as distance. We classified the chemicals into two kinds of clusters; their threshold values were $r = 0$ and $r = 0.408$ ($p < 0.01$), respectively. Gradient color indicates relative level (log transformed) of GI50. Red, more sensitive than the mean GI50 (2.0); yellow, mean GI50 (0.0); and green, less sensitive than the mean GI50 (−2.0). On the color scale, red represents the GI50 value that is 100-fold higher than the mean GI50.

NNK and SV-NN, on the other hand, belonged to the cluster D2. These results are in accordance with the similar fingerprints shown in Fig. 2. It is noteworthy that the snake venoms from the *C. atrox* and *T. flavoviridis*, species belonging to the viperidae family of snakes, formed another cluster (cluster D3), which was different from that of the elapidae family of snakes, *N. naja kaouthia* and *N. nigricollis*. 9-*cis* Retinoic acid, 13-*cis* retinoic acid, and 4-[*E*-2-(5,6,7,8-tetrahydro-5,5,8,8-tetra-methyl-2-naphthalenyl)-1-propenyl]benzoic acid, which are RAR agonists (Aström et al., 1990), also formed a separate cluster (cluster D1). Likewise, agricultural chemicals paraquat, ziram, and thiram formed a single cluster (cluster F1).

Discussion

The JFCR39 system coupled to a drug activity database is a good model for investigating the diversity of chemosensitivity in cancer cells. We have previously established panels of human cancer cell lines [JFCR39 (Yamori, 2003) and JFCR45 (Nakatsu et al., 2005)]. We used these panels of cells to demonstrate that they provide powerful means to predict the action mechanisms of drugs, and also used them to identify new target compounds. In this manuscript, we used the JFCR39 system to evaluate various chemicals (such as toxic chemicals, agricultural chemicals, and synthetic intermediates), which are not anticancer drugs, and classified them according to their molecular target or action mechanism. As a result, these chemicals were classified into a number of clusters. Our results also suggested that each cluster consisted of chemicals sharing a common action mechanism.

We determined the growth inhibition of cells in the JFCR39 panel by 130 chemicals and calculated their GI50 values. Some of the chemicals were assessed twice or more to confirm the reproducibility of the assay. We had to exclude 61 chemicals from further analysis because they did not inhibit the cells in the JFCR39 panel significantly. The rest of the chemicals (69 of 130, ~60%) met our selection criteria and were evaluated by cluster analysis.

First, we found that the chemicals tested in duplicate formed tight clusters, showing high reproducibility. Next, we investigated the difference between these 69 test chemicals and the anticancer drugs. Sixty-nine chemicals, which are not anticancer drugs, formed several clusters, which were different from the anticancer drug clusters. These results suggest that the action mechanisms of these chemicals are different from the action mechanisms of the anticancer drugs. However, we found that cisplatin did not belong to the cluster A, which consisted of DNA-targeting anticancer drugs. We do not understand the reason at present. However, there is a possibility that cisplatin has other action mechanisms, which may have made the fingerprint of cisplatin different from those of other DNA-targeting drugs. Indeed, cisplatin is known to form DNA-protein cross-links (Zwelling et al., 1979; Chválová et al., 2007).

Our analysis also identified several interesting clusters. For example, the cluster F3 consisted of cardiac glycosides digoxin and ouabain, both of which inhibit Na-K ATPase (Reuter et al., 2002). The cluster D1 consisted of 9-*cis* retinoic acid, 13-*cis* retinoic acid, and 4-[*E*-2-(5,6,7,8-tetrahydro-5,5,8,8-tetra-methyl-2-naphthalenyl)-1-propenyl]benzoic acid, which are RAR agonists. These results suggest that chemicals other than the anticancer drugs also form clusters when they share the same action mechanisms. It is noteworthy that SV-NNK and SV-NN, from snakes that belonged to the elapidae family, formed one cluster (cluster D2). In contrast, the snake venoms from the *C. atrox* and *T. flavoviridis*, which belonged to the viperidae family, formed a cluster (cluster D3) different from the elapidae cluster. These results are reasonable because snake venoms from different snake families are known to differ not only in composition but also in levels of toxicity and mechanisms of action.

The agricultural chemicals paraquat, ziram, and thiram were also classified into a single cluster (cluster F1). Among these agricultural chemicals, the action mechanism of ziram is not known. However, both paraquat and thiram are known to induce oxidative stress (Cereser et al., 2001; Suntres, 2002). Therefore, based on our observations, we could suggest that ziram also acted by inducing oxidative stress. The agricultural chemicals methoprene (insect growth regulator) and carbaryl (chorine esterase inhibitor) formed cluster L3, although their common mechanism is unknown. Cluster D4 and D5 consist of the antibacterial agents or fungicides. 3-Iodo-2-propynyl-butylcarbamate and *p*-chlorophenyl-3′-iodopropargylformal, belonging to cluster D4, are the iodo-type antibacterial agents.

Thus, cluster analysis of GI50 values of various chemicals, determined using the JFCR39 cell panel, suggests that the JFCR39 system could, at least in part, allow classification of chemical compounds on the basis of their action mechanisms. Our analysis also suggests that the chemicals belonging the same cluster share a common action mechanism. We are going to develop a larger library of reference chemicals with known action mechanisms (i.e., various inhibitors of biological pathways), and expand our database by integrating their GI50 measurements, which will make the cluster analysis as well as the COMPARE analysis more informative for predicting the mechanism of test chemicals.

In conclusion, to evaluate the potential of the JFCR39 system in predicting the action mechanisms of toxic chemicals, we investigated the fingerprints of 130 different types of chemical compounds including toxic chemicals, pesticides, drugs, and synthetic intermediates. Using the hierarchical clustering analysis, we classified 69 chemicals, at least in part, based on their action mechanisms. Thus, this approach using the JFCR39 cell panel is useful not only in predicting the action mechanisms of toxic chemicals but also in evaluating their toxicity.

Acknowledgments

We thank Yumiko Mukai, Yumiko Nishimura, and Mariko Seki for determination of chemosensitivity and Satoshi Kitajima for help with chemical information.

References

Akashi T, Nishimura Y, Wakatabe R, Shiwa M, and Yamori T (2007) Proteomics-based identification of biomarkers for predicting sensitivity to a PI3-kinase inhibitor in cancer. *Biochem Biophys Res Commun* **352**:514–521.

Akashi T and Yamori T (2007) A novel method for analyzing phosphoproteins using SELDI-TOF MS in combination with a series of recombinant proteins. *Proteomics* **7**:2350–2354.

Aström A, Pettersson U, Krust A, Chambon P, and Voorhees JJ (1990) Retinoic acid and synthetic analogs differentially activate retinoic acid receptor dependent transcription. *Biochem Biophys Res Commun* **173**:339–345.

Cereser C, Boget S, Parvaz P, and Revol A (2001) An evaluation of thiram toxicity on cultured human skin fibroblasts. *Toxicology* **162**:89–101.

Chválová K, Brabec V, and Kasparkova J (2007) Mechanism of the formation of DNA-protein cross-links by antitumor cisplatin. *Nucleic Acids Res* **35**:1812–1821.

Dan S, Shirakawa M, Mukai Y, Yoshida Y, Yamazaki K, Kawaguchi T, Matsuura M, Nakamura Y, and Yamori T (2003) Identification of candidate predictive markers of anticancer drug sensitivity using a panel of human cancer cell lines. *Cancer Sci* **94**:1074–1082.

Dan S, Tsunoda T, Kitahara O, Yanagawa R, Zembutsu H, Katagiri T, Yamazaki K, Nakamura Y, and Yamori T (2002) An integrated database of chemosensitivity to 55 anticancer drugs and gene expression profiles of 39 human cancer cell lines. *Cancer Res* **62**:1139–1147.

Hershberger LG, Shipley EG, and Meyer RK (1953) Myotrophic activity of 19-nortestosterone and other steroids determined by modified levator ani muscle method. *Proc Soc Exp Biol Med* **83**:175–180.

Jamieson ER and Lippard SJ (1999) Structure, Recognition, and Processing of Cisplatin-DNA Adducts. *Chem Rev* **99**:2467–2498.

Kanno J, Kato H, Iwata T, and Inoue T (2002) Phytoestrogen-low diet for endocrine disruptor studies. *J Agric Food Chem* **50**:3883–3885.

Naasani I, Seimiya H, Yamori T, and Tsuruo T (1999) FJ5002: a potent telomerase inhibitor identified by exploiting the disease-oriented screening program with COMPARE analysis. *Cancer Res* **59**:4004–4011.

Nakamura H, Dan S, Akashi T, Unno M, and Yamori T (2007) Absolute quantification of four isoforms of the class I phosphoinositide-3-kinase catalytic subunit by real-time RT-PCR. *Biol Pharm Bull* **30**:1181–1184.

Nakatsu N, Yoshida Y, Yamazaki K, Nakamura T, Dan S, Fukui Y, and Yamori T (2005) Chemosensitivity profile of cancer cell lines and identification of genes determining chemosensitivity by an integrated bioinformatical approach using cDNA arrays. *Mol Cancer Ther* **4**:399–412.

Okutsu J, Tsunoda T, Kaneta Y, Katagiri T, Kitahara O, Zembutsu H, Yanagawa R, Miyawaki S, Kuriyama K, Kubota N, et al. (2002) Prediction of chemosensitivity for patients with acute myeloid leukemia, according to expression levels of 28 genes selected by genome-wide complementary DNA microarray analysis. *Mol Cancer Ther* **1**:1035–1042.

Paull KD, Shoemaker RH, Hodes L, Monks A, Scudiero DA, Rubinstein L, Plowman J, and Boyd MR (1989) Display and analysis of patterns of differential activity of drugs against human tumor cell lines: development of mean graph and COMPARE algorithm. *J Natl Cancer Inst* **81**:1088–1092.

Reuter H, Henderson SA, Han T, Ross RS, Goldhaber JI, and Philipson KD (2002) The Na^+-Ca^{2+} exchanger is essential for the action of cardiac glycosides. *Circ Res* **90**:305–308.

Scherf U, Ross DT, Waltham M, Smith LH, Lee JK, Tanabe L, Kohn KW, Reinhold WC, Myers TG, Andrews DT, et al. (2000) A gene expression database for the molecular pharmacology of cancer. *Nat Genet* **24**:236–244.

Suntres ZE (2002) Role of antioxidants in paraquat toxicity. *Toxicology* **180**:65–77.

Weinstein JN, Kohn KW, Grever MR, Viswanadhan VN, Rubinstein LV, Monks AP, Scudiero DA, Welch L, Koutsoukos AD, and Chiausa AJ (1992) Neural computing in cancer drug development: predicting mechanism of action. *Science* **258**:447–451.

Weinstein JN, Myers TG, O'Connor PM, Friend SH, Fornace AJ Jr, Kohn KW, Fojo T, Bates SE, Rubinstein LV, Anderson NL, et al. (1997) An information-intensive approach to the molecular pharmacology of cancer. *Science* **275**:343–349.

Wong E and Giandomenico CM (1999) Current status of platinum-based antitumor drugs. *Chem Rev* **99**:2451–2466.

Yaguchi S, Fukui Y, Koshimizu I, Matsuno T, Gouda H, Hirono S, Yamazaki K, and Yamori T (2006) Antitumor activity of ZSTK474, a new phosphatidyl inositol 3-kinase inhibitor. *J Natl Cancer Inst* **98**:545–556.

Yamori T (2003) Panel of human cancer cell lines provides valuable database for drug discovery and bioinformatics. *Cancer Chemother Pharmacol* **52 (Suppl 1)**: S74–S79

Yamori T, Matsunaga A, Sato S, Yamazaki K, Komi A, Ishizu K, Mita I, Edatsugi H, Matsuba Y, Takezawa K, et al. (1999) Potent antitumor activity of MS-247, a novel DNA minor groove binder, evaluated by an in vitro and in vivo human cancer cell line panel. *Cancer Res* **59**:4042–4049,.

Zembutsu H, Ohnishi Y, Tsunoda T, Furukawa Y, Katagiri T, Ueyama Y, Tamaoki N, Nomura T, Kitahara O, Yanagawa R, et al. (2002) Genome-wide cDNA microarray screening to correlate gene expression profiles with sensitivity of 85 human cancer xenografts to anticancer drugs. *Cancer Res* **62**:518–527.

Zwelling LA, Anderson T, and Kohn KW (1979) DNA-protein and DNA interstrand cross-linking by cis- and trans-platinum(II) diamminedichloride in L1210 mouse leukemia cells and relation to cytotoxicity. *Cancer Res* **39**:365–369.

Address correspondence to: Takao Yamori, Division of Molecular Pharmacology, Cancer Chemotherapy Center, Japanese Foundation for Cancer Research, 3-10-6, Ariake, Koto-ku, Tokyo 135-8550, Japan. E-mail: yamori@jfcr.or.jp, 07a$sl